



Micro-seismic hazard assessment of Ahmedabad city, Gujarat (Western India) through near-surface characterization/soil modeling

Kapil Mohan, et al. [full author details at the end of the article]

Received: 7 November 2019 / Accepted: 10 December 2020 / Published online: 3 January 2021
© The Author(s), under exclusive licence to Springer Nature B.V. part of Springer Nature 2021

Abstract

The micro-seismic hazard estimation including quantification of the ground motion amplification has been conducted at Ahmedabad city based on near-surface characterization/soil modeling. The city has experienced substantial damage in the course of the 2001 Bhuj earthquake. A total of 20 boreholes were drilled in the city up to the depths of 40–80 m. A five-fold methodology is adopted: (1) Assessment of the seismic perspective of the area under study, (2) demarcation of the engineering bed layer (EBL) through geophysical (seismic) surveys and the soil properties, (3) soil modeling using geotechnical and the geophysical parameters, (4) assessment of the strong ground motion at EBL through simulation considering far-field earthquake scenarios and near-field earthquakes scenario and (5) surface strong-motion estimation by ground response analysis based on equivalent-linear approach. The near-surface soil models were prepared from the borehole logs, shear-wave velocity estimated from the seismic survey and the soil properties like soil classification and density. The strong motion at EBL is computed by simulating seismotectonically justified scenario earthquakes through the stochastic finite-fault source modeling technique using the region-specific input parameters. The surface-strong motion is estimated by performing ground response analysis (with SHAKE) at every borehole using EBL-strong motion and prepared soil models. The EBL was found varying from 28 to 54 m in depth in Ahmedabad city. The effect of far-field and near-field earthquake sources was considered for assessing the hazard. To compensate for the uncertainty, a total of 108 and 81 input parametric combinations for near-field earthquake scenarios, and far-field earthquake scenarios, respectively have been considered for estimating the strong motion at EBL. The peak ground acceleration (PGA) of 52–111 cm/s^2 and 108 cm/s^2 are estimated at EBL due to near-field earthquake scenarios and far-field earthquake scenarios, respectively. The PGA through ground response analysis at surface level is found to be varying from 101 to 279 cm/s^2 for near-field earthquake scenarios and, 118–161 cm/s^2 for the far-field earthquake scenarios. The spectral acceleration (SA) (at surface level) has also been calculated for damping of 5%. The average SA distribution maps for 0.2 s (1–2 story), 0.55 s (4–5 story), 1 s (high rise) and 1.25 s period (large structures) have been prepared for both types

Supplementary Information The online version contains supplementary material available at (<https://doi.org/10.1007/s10518-020-01020-w>).

of scenario earthquakes. The strong motion amplification is computed to be in the range of 1.6–3.3 for near-field earthquake scenarios and 2.2–3.0 for near-field earthquake scenarios.

Keywords Micro-seismic hazard · Geophysical and geotechnical parameters · Scenario earthquakes · Ground response analysis · Site effects · Ground motion amplification

1 Introduction

The unpredictability and severity of earthquakes classify them as the most dangerous natural hazards. Approximately 1.5–2.0 million people have lost their lives in 1000 deadly earthquakes recorded in the last century (Pomonis et al. 1993) whereas, over 200 fatal earthquakes have been experienced in the 21st century with a total loss of life of more than 0.7 million people [United State Geological Survey (USGS)]. The destruction due to such an event (in the future) can be minimized by reducing their effects through precise seismic hazard assessment and incorporating it in seismic designing. With the increase of population, the danger gets higher in many earthquake-susceptible regions, especially in growing nations, like Nepal, India, Haiti, etc. The Ahmedabad city falls in the central-eastern part of Gujarat state of India. It also falls under seismic zone III of the Indian seismic zone map of India (BIS: 1893–2016), The Gujarat state has experienced two large earthquakes; the 1819 Allah Bund Earthquake of magnitude 7.8 and the 2001 Bhuj Earthquake of magnitude 7.6 (2001 Bhuj Eq.) and several other earthquakes of magnitude ≤ 6 in the last 100 years (Rastogi et al. 2012). It is still seismically active.

Ahmedabad is the major city and the former capital of Gujarat. It is situated 32 km SW of the present capital city, Gandhinagar. The city is categorized in zone III in the Indian seismic zone map. The city is located in the rift basin named Cambay rift formed by the West Cambay and East Cambay boundary faults which are dipping towards the city (Wani and Kundu 1995). Ahmedabad is a rapidly developing city in the state of Gujarat; the population is in a rising trend, which has led to continuous horizontal and vertical development. The city suffered heavily in the 2001 Bhuj Eq., even though the epicenter was 250 km away and the depth of the earthquake was ~ 25 km. Many high-rise structures had damaged (Mishra 2004). The city has also experienced an earthquake of Mw 5.7 in 1864, with an epicenter ~ 80 km south (ISR 2013). The past seismicity suggests the vulnerability of structures from large earthquakes in the future (both from near- and far-sources) and emphasizes the need for micro-seismic hazard assessment first of Ahmedabad city. The microzonation of the urban area (both residential and industrial) was practiced, in 1954, at the Yokohama city of Japan. Worldwide, seismic microzonation is carried out in several countries, like Japan (Yokohama, Urmia, and Tokyo), United States (Central US), Nepal (Kathmandu), Australia (Perth), China (Hong Kong) and India. In India, micro-seismic hazard assessment was carried out in metropolitan cities such as Delhi (Sharma and Rao 2004), Guwahati and Sikkim (Nath et al. 2008), Bangalore (Anbazhagan and Sitharam 2008), Chennai (Ganpathy 2011) and Jabalpur (Rao 2014). The macro-SHA work was carried out by many researchers in parts (Peterson et al. 2004; Iyengar and Raghukanth 2006; Chopra et al. 2012b, a; Mohan 2014) in Gujarat. The predominant frequency was estimated by Mandal et al. (2005) through the H/V method in the central-eastern Kachchh. On a national scale, Parvez et al. (2003) have prepared the deterministic seismic hazard assessment map of India. National Disaster Management Authority (NDMA 2010) has also proposed a probabilistic seismic hazard map of India on NEHRP-A- site class (with Vs30

≥ 1.5 km/s). Sitharam and Kolthiar (2013) have proposed the seismic hazard analysis of India using the areal sources. On a regional level, Chopra et al. (2012b, a) have carried out the Deterministic seismic hazard map of Gujarat in which surface PGA in Ahmedabad city is estimated. Bhandari et al. (2013) have also conducted a regional probabilistic seismic hazard assessment study in Ahmedabad. At the local level, the Gujarat State Disaster Management Authority, along with the Institute of Seismological Research and OYO International Corporation, Japan has conducted seismic microzonation in the Gandhidham-Kandla area, considering the tectonics, shear-wave velocity, and geotechnical data. Considering the geophysical, geological and geotechnical aspects, a micro-seismic hazard assessment of Ahmedabad is yet to be done.

In this work, we carried out a micro-level seismic hazard assessment in Ahmedabad through subsurface characterization using geotechnical and geophysical data. The strong motion data of large earthquakes is scarce in the study area to aid earthquake-resistant designing. In view of this, the strong motion due to large earthquakes is simulated by considering past seismicity, tectonic setting and various geotechnical, geophysical, and geological parameters. To recompense for the uncertainty, region-specific parameters are used and diverse scenarios are generated for near-field as well as far-field earthquakes. The local site effects are also incorporated by 1D-ground response analysis at each borehole location.

2 Geology and tectonic setting

The Ahmedabad city is located in a Cambay rift, formed in the early Cretaceous (Biswas 1982, 1987), with east and West Cambay margin faults as the rift shoulders (Fig. 1). The development of the Cambay rift, especially tectonic, is closely associated with the development in the Indian Plate (Biswas et al. 1994). The rifting propagated from east to west. The first rift stage started with extensional faulting from the east along the NNW–SSE older-Aravalli trend developing an easterly tilted half-graben in which the deltaic clastics had deposited. This was followed by widespread volcanism which was a syn-rift event and the effects of rifting were subdued by outpouring basaltic lava, resulting in the cover of a very thick lava pile over the Cretaceous sediments, which formed the basement of the Tertiary deposits in the second rift cycle. The basin evolved fully during the later cycle when the graben subsided by the extensional faulting to accommodate the huge thickness of marine/lagoonal fine clastic sediments from Late Paleocene to Mid-Miocene till the rifting process ceased (Biswas 1999). The Cambay basin extends broadly in an NNW–SSE direction in the onshore and the offshore parts of Gujarat (Fig. 1). The basin width narrows down towards the northern part, indicating a possible decline of the rift propagation. Northward, it swings to NE merging into the Rajasthan basin (Mehr and Chamyal 1997). oil and natural gas corporation (ONGC) through acquired and analysed data from the geophysical survey (mainly on the Tertiary sediments), revealed the basement configuration and delineated the cross faults that were responsible for the division of basin into sub-basins/tectonic blocks. These faults behaved differently during the deposition due to differential uplifts along with various bounding and transverse faults (Wani and Kundu 1995).

The faulted basin is filled with approximate 4000 m thick sediments of Tertiary to Quaternary in age. Based on the subsurface drilling and detail seismic surveys, ONGC (Biswas 1982; Wani and Kundu 1995) inferred different faults and depths to different geological layers. Due to the alluvial cover, these faults could be potentially detected

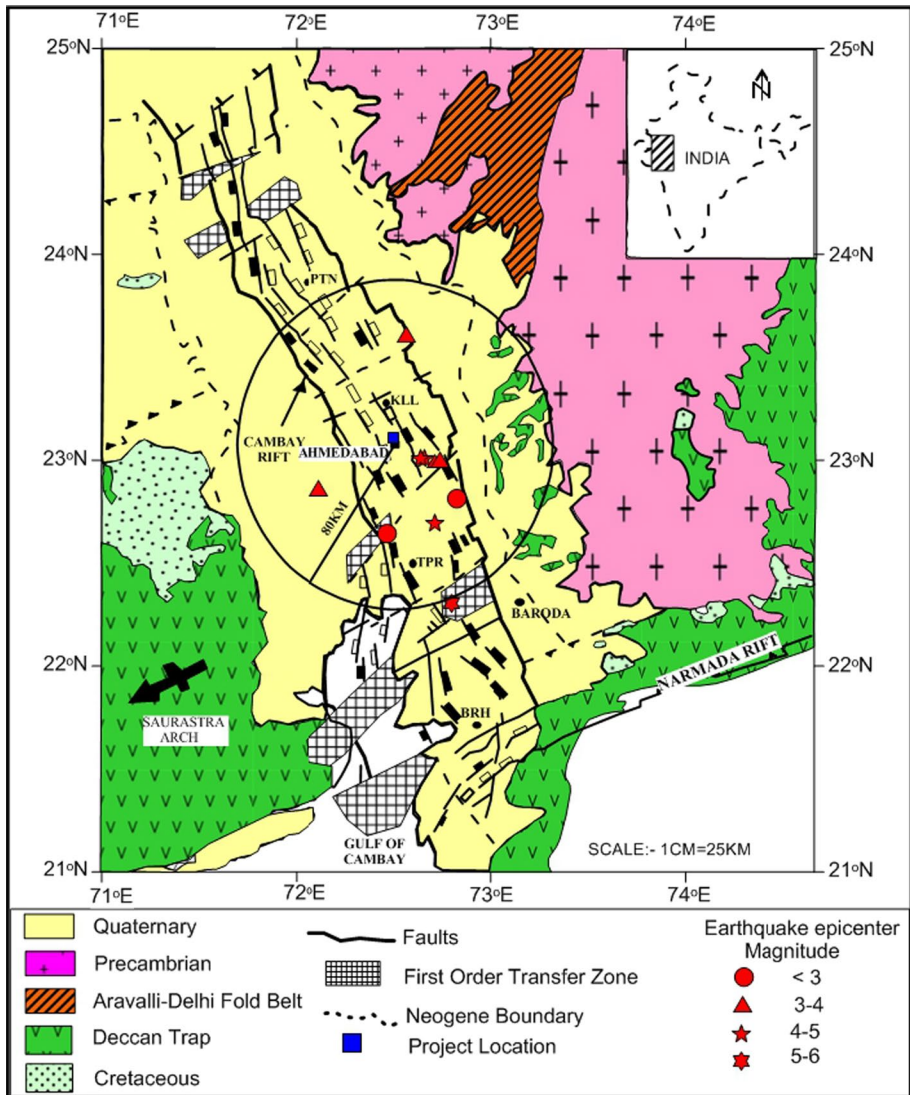


Fig. 1 Geology and structural map of Cambay rift basin (after Wani and Kundu 1995) overlapped with the seismicity up to 50 miles from the year 1668 to 2012

by geophysical surveys as these are not always easy to decipher (Dixit et al. 2010; Mohan et al. 2017a, b; Danda et al. 2017).

The city of Ahmedabad is situated on the banks of Sabarmati River, within 50 km wide Cambay basin (Fig. 1), enclosed by two NNE–SSW trending faults: West Cambay and East Cambay Faults.

3 Methodology

The present study is targeted to conduct a micro-seismic hazard assessment and to predict surface ground motion parameters for the Ahmedabad city through characterizing the near-surface. The entire scheme is divided into five main parts: the methodology proposed in the Mohan et al. (2017a, b, 2018) is considered in the current study. The estimation of surface strong ground motion is divided into five major parts:

- (1) Assessment of earthquake potential of the study area based on past seismicity and major tectonics.
- (2) Demarcation of the engineering bed layer (EBL) (in case if bedrock is deeper). The layer is marked based on a geotechnical property (SPT N value > 80), geophysical property ($400 \text{ m/s} \leq V_s \leq 750 \text{ m/s}$) and uniform distribution of soil type in the study area.
- (3) Preparation of soil models (soil modeling) using the geotechnical and geophysical parameters.
- (4) Assessment of the strong motion at EBL through simulation considering far-field and near-field earthquake scenarios using region-specific ground motion parameters.
- (5) Equivalent linear 1D-ground response analysis for the computation of strong motion at the surface. The flowchart showing methodology has been given in Fig. 2.

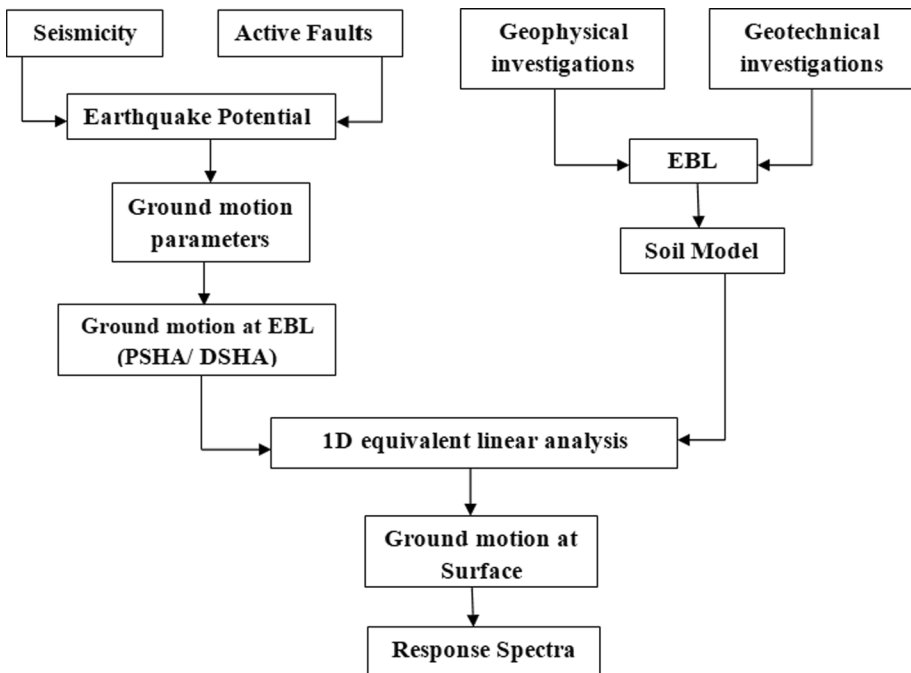


Fig. 2 The flow-chart showing methodology of estimation of SGM at the surface level

3.1 Estimation of the earthquake potential of the study area

The BIS classified the Ahmedabad city under seismic zone III (BIS 2016). The historical seismicity map prepared from the catalog of the Institute of Seismological Research, Gandhinagar suggests very few earthquakes in the vicinity of Ahmedabad city. A total of 26 earthquakes were observed in Ahmedabad city from 1821 to 2016 with the maximum magnitude of M5.7 that occurred in 1864. The Frequency–Magnitude range plot of the earthquakes has been shown in Fig. 3. Besides local earthquakes, Ahmedabad has also experienced large earthquakes from the Kachchh region. During the 2001 Bhuj earthquake, several multi-story reinforced concrete-frame buildings collapsed in Ahmedabad [80 buildings with 1021 apartments and 82 other houses collapsed (Mishra 2004)]. In total, 1103 units or families were affected by the collapsed structures in the city (Mishra 2004).

For designing earthquake-resistant structures, it is important to predict the expected peak accelerations during strong earthquakes. The buildings can be of different types; low story (1–4 story), mid-story (4–7 story) and high-rise (> 7 stories) buildings. The near-field earthquakes possess most of the energy in the high frequency/low period range. Therefore, near-field earthquakes are critical for low story buildings. Similarly, due to the low frequency/high period, the far-field earthquakes were found more critical for mid-rise and high-rise buildings. The East Cambay Boundary Fault has the potential of $M \leq 6$ earthquake (Rastogi 2014). Therefore, based on recent past experience of the 2001 Bhuj

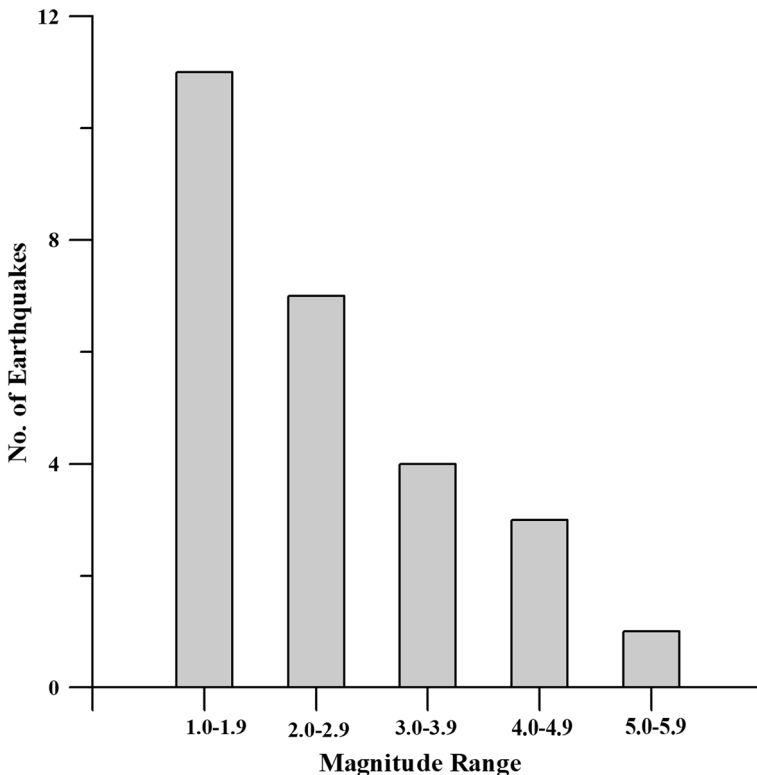


Fig. 3 Frequency–Magnitude plot of the Ahmedabad seismicity from 1821 to 2016

Earthquake, the seismic potential of the Eastern Cambay Boundary fault and the presence of low, mid and high-rise buildings in Ahmedabad, the near-field and far-field earthquake scenarios are considered for this study.

3.2 Establishment of EBL from geotechnical and geophysical data

3.2.1 Geotechnical investigations

Twenty boreholes were drilled in the Ahmedabad city up to the depths of 80 m (10 boreholes; BH-01–BH-10), 50 m (one borehole; BH-20) and 40 m (nine boreholes; BH-11–BH-19). The lithology of the boreholes drilled up to the depth of 80 m is given in Fig. 4.

The clay is present at the surface in the western and southeastern part of Ahmedabad city whereas the rest of the city is covered by the sand at the surface (Fig. 5). The North-east–Southwest and East–West soil cross-sectional profiles (locations marked in Fig. 5a) are shown in Fig. 5b and c, respectively.

The alternate layers of sandy and clayey units with more stiffness were found up to 20 m depth, denser 20 m onwards. At shallower depths of around 10 m, the corrected N-values reach > 50 (Very stiff/ Refusal), while at deeper depths the values reach > 100 (as same as a rock) (Sairam et al. 2018).

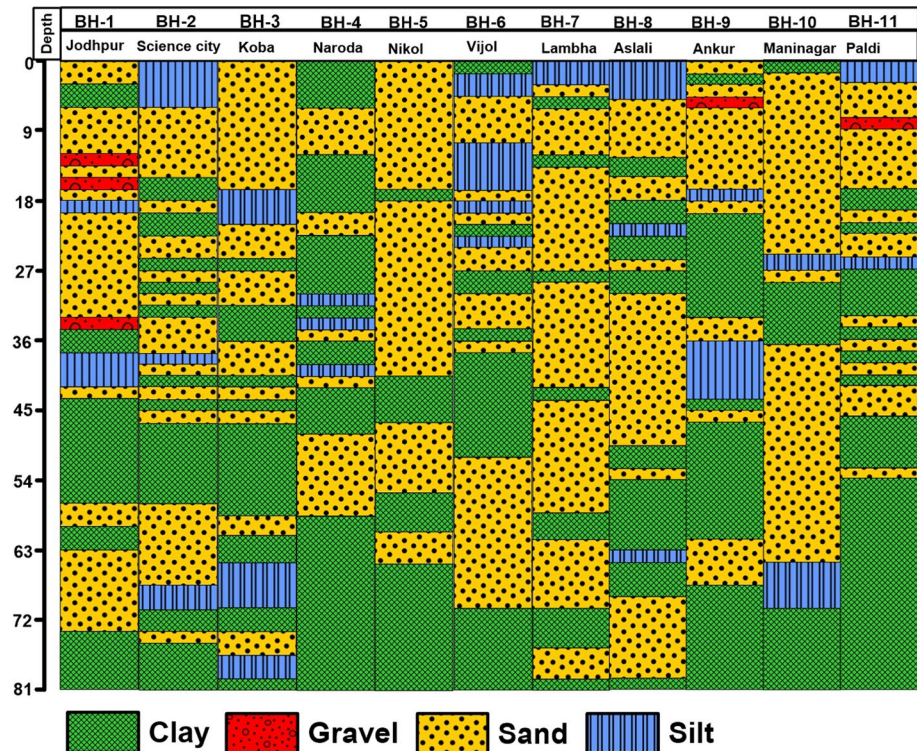


Fig. 4 Lithologies of the 11 boreholes drilled up to the depth of ~ 80 m in the Ahmedabad city

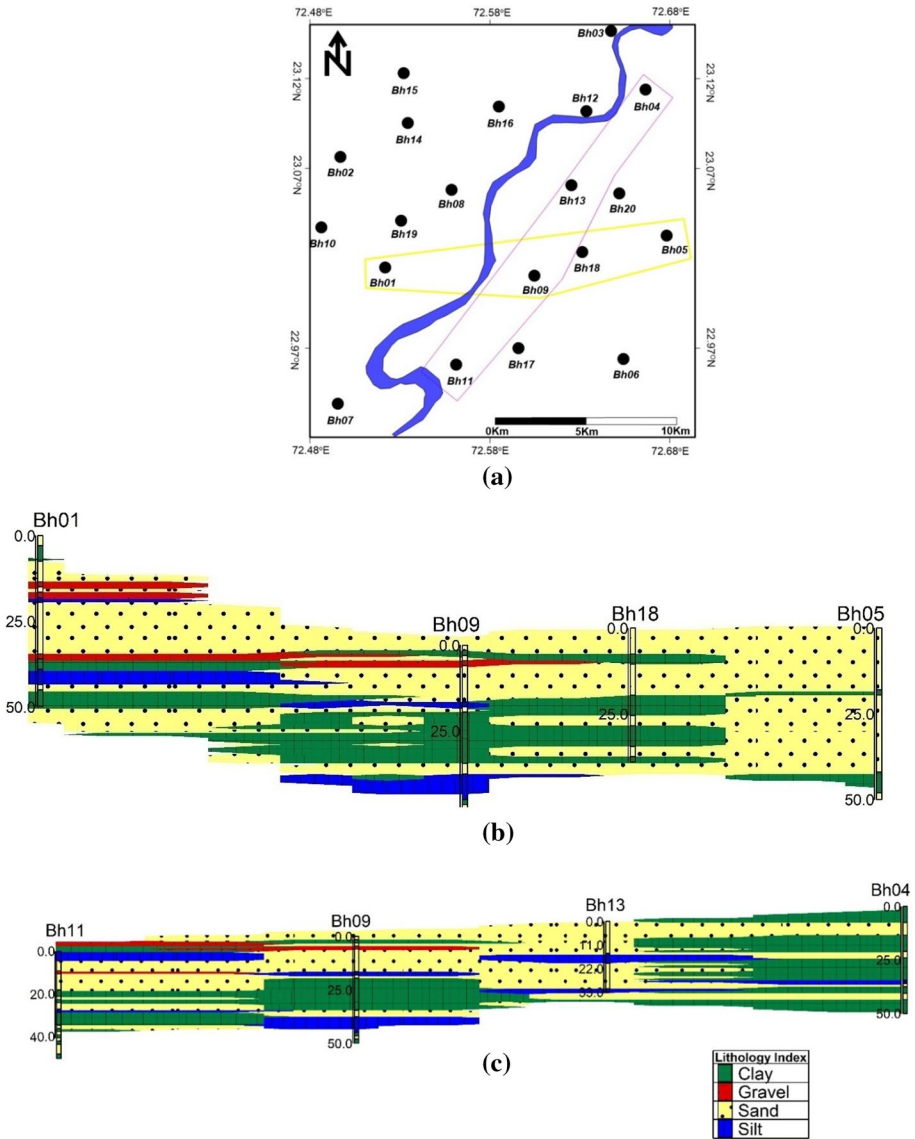


Fig. 5 a Location map of the soil profiles prepared in Ahmedabad City, b East–West soil Profile and c NE–SW Profile

- (6) These layers are classified as per the engineering geological classification based on average values of soil properties obtained from laboratory tests according to Indian Standards.

3.2.2 Geophysical investigations

In Ahmedabad, the shear-wave velocity (V_s) was estimated at 55 sites (having length of 60 m) using Multichannel Analysis of Surface Wave and at 11 sites with the PS-logging (Sairam et al. 2018) (Fig. 6). A good match of shear wave velocity (1D models) has been found at sites where both MASW and PS logging has been conducted. The V_{s30} was computed at each site (Sairam et al. 2018). The eastern portion adjacent to the Sabarmati River has shown higher velocity (300–360 m/s) than the western side (265–300 m/s). Only one site has shown a V_{s30} of about ~ 2005 m/s and two sites have shown the V_{s30} of ~ 380 m/s. On average, the V_{s30} has been found varying from 265 to 360 m/s (Fig. 6) in the Ahmedabad city and can be categorized in D-type soil (stiff soil) in the national earthquake hazards reduction program (NEHRP 2003) scheme. The two sites that showed higher V_{s30} can be classified as C-type soil (dense soil).

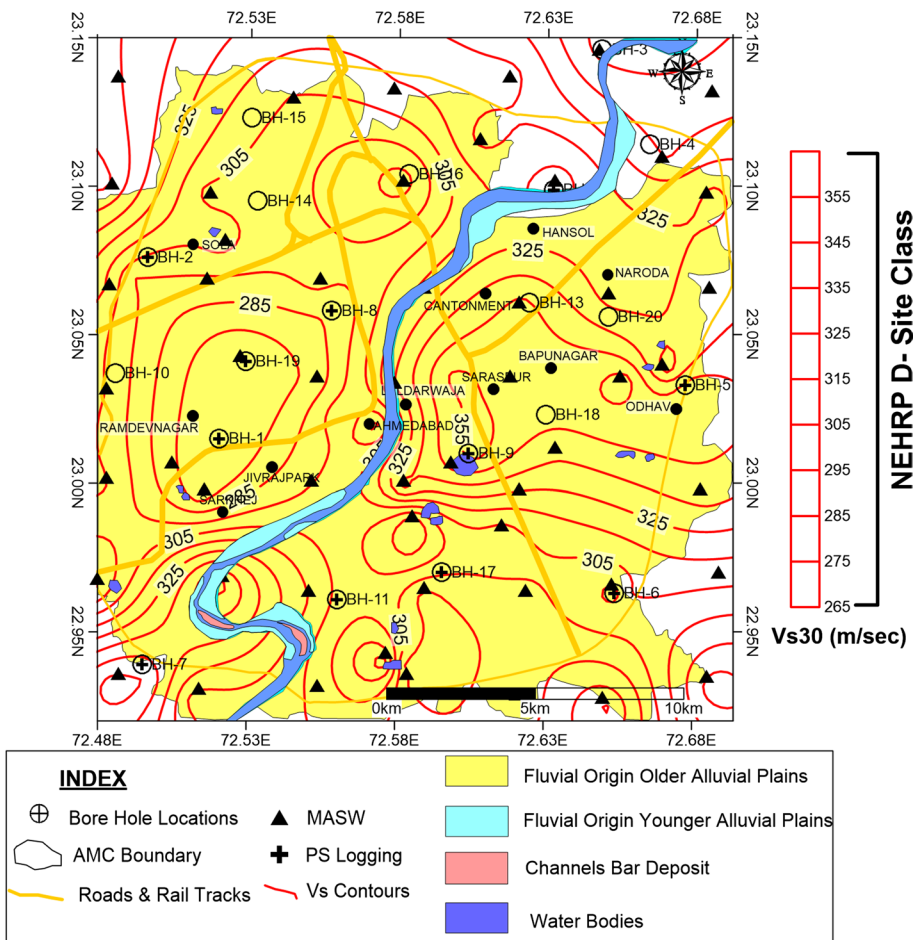


Fig. 6 The V_{s30} distribution map of Ahmedabad City prepared based on V_{s30} data from Sairam et al. (2018). The V_{s30} values vary from 265 to 360 m/s fall under the category of NEHRP D-site class (stiff soil)

Based on the seismic survey, Kaila et al. (1990) have suggested the deep basement/bedrock (of up to ~ 6 km) in Ahmedabad city, which is located in the Cambay rift. Therefore, the site effect on the strong motion can be estimated considering the engineering bed layer (EBL) in place of basement/bedrock. The shear wave velocity estimated through MASW survey and PS logging (Sairam et al. 2018) has shown a layer with $V_s \sim 500$ m/s in the Holocene sediments in the entire city. At similar depths, the geotechnical investigation from the boreholes has shown a layer with an N-value of more than 80 blow counts. Therefore, this layer (with a V_s of 500 m/s and N-value of ~ 80 blow counts) and present in the entire city has been considered as the engineering bed layer. The EBL is demarcated at about 24–54 m depth in Ahmedabad city. The depth of the EBL in Ahmedabad city is variable, being shallower (24–35 m) (in the west-central part and deeper (44–54 m) in the central and the south-eastern parts (Fig. 7 and Table 1).

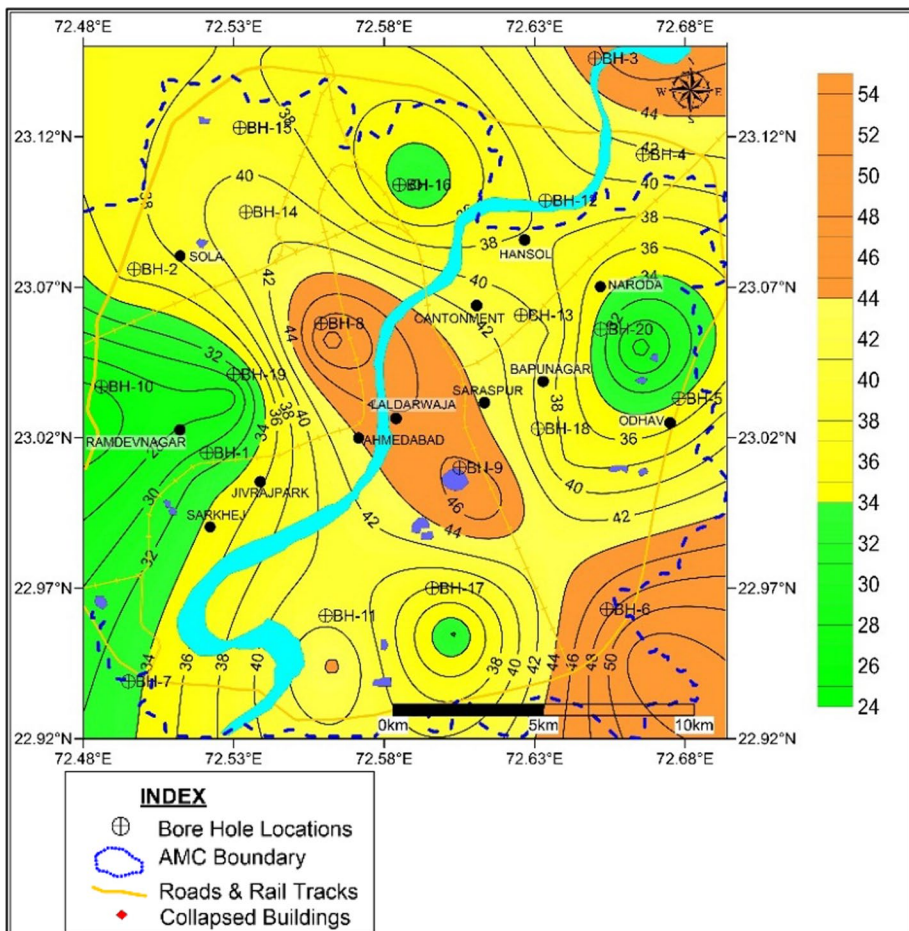


Fig. 7 EBL distribution in the Ahmedabad City

Table 1 The depth of EBL demarcated in different boreholes based on geophysical survey and geotechnical testing

BH no.	EBL Depth (m)	BH no.	EBL depth (m)
BH-01	33.0	BH-11	44.5
BH-02	36.0	BH-12	39.0
BH-03	48.0	BH-13	40.0
BH-04	42.0	BH-14	41.8
BH-05	39.0	BH-15	38.5
BH-06	54.0	BH-16	31.5
BH-07	33.0	BH-17	31.5
BH-08	51.0	BH-18	37.5
BH-09	48.0	BH-19	27.0
BH-10	24.0	BH-20	27.0

3.3 Soil modeling

A total of 20 boreholes were drilled in the Ahmedabad city: 10 boreholes are drilled up to 80 m depth (BH-01–BH-10), one borehole (BH-20) up to 50 m depth and 9 boreholes up to 40 m depth (BH-11–BH-19). The lithology is classified based on the grain size analysis (maximum content of clay, silt or sand) for the soil modeling. If any of the soil types (Gravel, Clay, Sand, or Silt) occupies > 50% of the soil, then the soil is designated as that type of soil. In case, all soil types show < 50% presence, then the soil (Sand, Silt, Clay or Gravel with the highest presence is designated as the soil type.

Based on the soil investigation from geotechnical data and geophysical investigations, soil models of 20 boreholes were prepared for the ground response analysis. The properties like wet density, N-value, plasticity index estimated from the borehole data and V_s (estimated through MASW survey and PS logging) have been considered to model the soil. The depth of the groundwater table (estimated from borehole drilling in the city) is found to vary from 8 m to more than 30 m in the city and is considered for preparing soil models. The prepared soil models for the boreholes BH-01 and 08 are given in Tables 2 and 3, respectively. A 3–18 m thick clay has been found (from the surface) in the Ahmedabad city, west to Sabarmati River and in the SE part, whereas sand covers (2–30 m) the rest of the city, east to the river. The remaining soil models (18 nos.) have been given as supplementary information.

Table 2 The Soil model prepared for the borehole BH-01

Depth	Thickness	Wet density (g/cc)	Soil type	PI	$(N_1)_{60}$	V_s
3	3	1.94	Clay	0	10	127
6	3	1.70	Clay	18	15	221
9	3	1.52	Sand	–	30	288
12	3	1.31	Sand	–	43	280
18	3	1.78	Sand	–	79	553
21	3	1.52	Sand	–	80	557
27	6	1.85	Sand	–	77	614
33	6	1.80	Sand	–	95	742
		1.85	EBL			590

Table 3 The Soil model prepared for the borehole BH-08

Depth	Thickness	Wet density(g/cc)	Soil Type	PI	(N ₁) ₆₀	V _s
3	3	1.31	Clay	19	12	204
6	3	1.38	Sand	–	11	233
15	9	1.58	Sand	–	29	357
24	9	1.67	Clay	21	33	377
27	3	1.47	Clay	18	63	276
33	6	1.54	Clay	29	90	544
36	3	1.62	Sand	–	90	392
42	6	1.59	Clay	23	Refusal	486
45	3	1.45	Clay	24	Refusal	526
48	3	1.46	Clay	16	Refusal	468
51	3	1.79	Sand	–	Refusal	417
		1.84	EBL		Refusal	550

3.4 Estimation of strong motion at EBL

Aki (1966, 1967) proposed an expression for a seismic wave spectrum radiated from complex faulting and correlated the seismic moment to the rigidity, slip, and fault area. The concept was used for ground motion estimation for high frequencies. Hartzell (1978) proposed the concept of division of rupture along a finite fault into sub-faults/sub-sources. These sub-faults can be deliberated as a point source. The concept covered the distributed and inhomogeneous rupture and the effect of the geometry of the fault. In this concept, the resultant strong motion is assessed at a site by summation of the contribution of sub-sources considering the time delays of sub-sources due to propagation of the rupture and source to site distance. This concept was further followed by Irikura (1983, 1992); Midorikawa (1993); Irikura and Kamae (1994). Beresnev and Atkinson (1998a) implemented the concept of a stochastic approach in the strong motion simulation by dividing the fault into sub faults considered as sub-sources that follows the ω^2 source spectrum. The systematically delayed sub-source effects were then included in the time-domain to estimate the strong motion at the interested site. The prepared source code was named FINSIM (Beresnev and Atkinson 1998b); Motazedian and Atkinson (2005) have further modified this source code by introducing the theory of dynamic corner frequency. In this concept, the corner frequency is assumed as a function of time and the total energy emitted from the fault is independent of sub source size unlike the static corner frequency (Motazedian and Atkinson 2005). The modified approach, therefore, is very less dependent on the sub-source size. This approach is named as stochastic finite fault modeling technique (SFFMT) for strong motion simulation. The revised source code is named as EXSIM. In the Stochastic finite fault modeling technique, the rupture history controls the frequency content of the simulated time series of each sub-fault. The advantage of the modified stochastic finite fault model is that it conserves moment with the single triggering of each sub-fault as compared to multiple triggering in previous approaches (e.g. Silva and Darragh 1995; Beresnev and Atkinson 1998a). In the current work, strong motion is simulated at the EBL using the stochastic finite fault modeling technique. This method was successfully applied to simulate strong motion in various parts of the world. The detail has been given

Table 4 The List of simulated earthquakes worldwide using Stochastic Finite Fault modeling Technique (Motazedian and Atkinson 2005)

Sr. No.	Earthquake	References
1	1992, Landers earthquake of M 7.2	Motazedian and Atkinson(2005)
2	2003, Bam, Iran earthquake of M 6.5	Motazedian and Moinfar (2006)
3	1999, Düzce (Turkey) Earthquake	Ugurhan and Askan (2010)
4	M 7.4 Scenario earthquake in Istanbul, Turkey	Zengin and Cakti (2012)
5	2016 Meinong, Taiwan earthquake	Chen et al. (2017)
6	2015, Gorkha, Nepal earthquake of Mw 7.8	Raghucharan and Somala (2017)
7	2001, Bhuj, India earthquake of Mw 7.6	Chopra et al. (2010)
8	Scenario Great earthquake in Himalaya	Chopra et al. (2012b, a)
9	Mw 7.6 and 7.5 scenario earthquakes in coastal zone of Gujarat, India	Mohan et al. (2017a, b)
10	Mw 7.6 and Mw6.0 scenario earthquakes in Gandhinagar, Gujarat, Indiar	Mohan et al. (2018)

in Table 4. The requirement of two types of scenario earthquakes has been deliberated in the current study (1) near-field earthquake scenarios and (2) far-field earthquake scenarios. Input strong motion is simulated at EBL using stochastic finite fault modeling technique of Motazedian and Atkinson (2005) at Vs of 500 m/s. The requirement of two types of scenario earthquakes has been deliberated in the current study (1) near-field earthquake scenarios and (2) far-field earthquake scenarios. Input strong motion is simulated at EBL using the stochastic finite fault modeling technique of Motazedian and Atkinson (2005) at EBL (Vs of 500 m/s).

3.4.1 Input parameters for simulation of strong motion at EBL

In the historic past, Ahmedabad city has experienced two earthquakes of magnitudes 3.7 (in 1843 and 1897), one of 4.6 (in 1840) and one of 5.7 (in 1864) (Oldham 1883). Several other small shocks were also experienced in and around Ahmedabad (ISR 2013). Besides, large earthquakes that occurred in Kachchh district (Mw 6, 1956 Anjar earthquake 2001 Bhuj Eq. and 1819- ABEQ), at a distance of ~ 250 km from the city, had affected Ahmedabad. Several multi-story reinforced concrete-frame buildings were collapsed in Ahmedabad (Mishra 2004). The famous minaret of Jama Masjid (mosque) located in Ahmedabad was damaged during the 1819-ABEQ that occurred in the NW part of Kachchh, Gujarat (Martin and Szeliga 2010).

For proper designing of earthquake-resistant structures, it is important to estimate the level of accelerations expected during future large earthquakes. Ahmedabad has experienced the effect of both near-field and far-field sources in the past and has low-story, mid-story, and high rise buildings. Therefore, consideration of both the sources (near-field as well as far-field) become essential for the estimation of possible seismic hazard of the city. The unavailability of strong motion recordings in low seismicity areas suggests the simulation with well-justified input parameters (seismological, geophysical, geological and geo-technical) as the alternate option.

The Cambay rift is enclosed by the West Cambay Boundary fault and East Cambay Boundary fault (Fig. 1). In 1864, an earthquake of magnitude M5.7 occurred along the

East Cambay Boundary fault. This fault with a dip of 60° has the potential to generate an earthquake of $M \leq 6$ (Rastogi 2014). Thus, near-field scenario earthquakes of magnitudes M_w 5.5, 6.0 and 6.5 (at the maximum) have been considered along this fault. Wells and Coppersmith (1994) have proposed relations to estimate the rupture dimensions based on worldwide dataset. The same relations have been used to estimate rupture dimensions in the present study. The West Cambay Boundary fault is an NNW–SSE trending fault that has a strike direction of 330° and dips of around 60° (Wani and Kundu 1995). So, for near-field, two scenarios are considered, one from ECF and another from WCF.

The M_w 7.6, 2001 Bhuj earthquake was located ~ 250 km NW of Ahmedabad. Also, M_w 7.8, 1819 Allah Bund earthquake occurred ~ 270 km from the city. Effectively, earthquakes with M_w 7.0, 7.8 and 7.6 have been considered for the far-field earthquake scenarios. The Wells and Coppersmith (1994) relationship has been used to estimate the rupture dimension for M_w 7.0 and 7.8 scenario earthquakes and the rupture dimensions proposed by Yagi and Kikuchi (2001) for 2001 BEQ have been considered for simulation of M_w 7.6. The quality factor proposed by Chopra et al. (2010) and Gupta et al. (2012) from local earthquakes has been used for compensating the path effect for near-field earthquake scenarios. The quality factor estimated by Singh et al. (1999, 2004) and Bodin et al. (2004) are used for the far-field earthquake scenarios. The Kappa values (κ), which takes into account the near-surface wave attenuation/Fall-off of the high frequency (> 1 Hz) Fourier amplitude spectrum (Anderson and Hough 1984) was considered around 0.03 for areas covered by Quaternary alluvium (Rapolu and Mandal 2014; Kumar 2015; Chandler et al. 2006). We took Kappa values of 0.02, 0.025 and 0.03 for the present work.

The stress values for shallow earthquakes of the stable continental region (M_w 6.7 Koyna earthquake in 1967, M_w 5.7 Bhadrachalam earthquake in 1969, and M_w 5.4 Broach earthquake in 1970) is around 60 bars (Rastogi 2016). Therefore, stress drop values of 60, 80 and 100 bars have been used in the near-field scenario earthquakes. Bodin and Horton (2004) computed the stress drop of 160 bars for the 2001 Bhuj Eq. thus, a stress drops of 140, 160, and 180 bars have been used for the far-field earthquake scenarios.

The strong motion due to near-field earthquake scenarios (M_w 5.5, 6.0 and 6.5 at East Cambay Boundary fault and far-field Eqs. (M_w 7, 7.6 and 7.8 at the eastern part of KMF) are generated using model parameters as shown in Tables 5 and 6, respectively and considering site amplifications suggested by Boore and Joyner (1997) for generic soils at V_s30 (average V_s in top 30 m subsurface layer) of 520 m/s (Table 7). Although it is not possible to predict earthquakes but the seismic scenarios based on past seismicity and estimated source parameters of the past earthquakes in the area can provide a reasonable seismic hazard for the region. Therefore, a total of 108 and 81 input parametric combinations have been considered for estimating the strong motions at EBL for near-field and far-field earthquake scenarios, respectively.

3.5 Ground response analysis

The equivalent-linear ground response analysis is a popular technique of estimation of ground response due to an earthquake. Therefore, it has been applied at each borehole site to estimate the surface strong motion. In the equivalent-linear analysis, the transfer functions are computed for a horizontally polarized vertically propagating shear wave passing through a soil column with layers of different stiffness, frequency, density and damping. Initially, the small values of strain, damping, and stiffness are considered for obtaining the response of the soil column. From this initial estimate, shear strain for

Table 5 The selected model parameters for simulation of SGM due to near-field earthquake scenarios

Magnitude (Mw)	5.5, 6.0 and 6.5
Fault length and width (km)	(7 km and 6 km), (13 km and 9 km), and (23 km and 14 km) Wells and Coppersmith (1994)
Strike and dip	330° and 60° (West Cambay Fault) 180° and 60° (East Cambay Fault)
Slip distribution	Random
Shear wave velocity	3.6 km/s
Density	2.8 gm/cm ³
Stress drop	60, 80 and 100 bars
Kappa	0.02, 0.025, 0.03
Anelastic attenuation Q(f)	149f ^{1.43} , 112f ^{0.94} Chopra et al. (2010), Gupta et al. (2012)
Geometric spreading	1/R (R ≤ 40 km) Bodin et al. (2004) 1/R ^{0.5} (40 ≤ R ≤ 80 km) 1/R ^{0.55} (R ≥ 80 km)
Duration properties	f _c ⁻¹ (R < 10 km) Eastern North America f _c ⁻¹ + 0.16R (10 ≤ R ≤ 70 km) Atkinson and Boore (1995) f _c ⁻¹ - 0.03 (70 < R ≤ 130 km) f _c ⁻¹ + 0.04R (130 < R < 1000 km)
Pulsing percent	50%

every layer is computed. Then, for each layer, the effective shear strain (which is magnitude dependent) is calculated as some part of the maximum shear strain. In the present study, it is (taken as 0.65 due to the considered scenario earthquake of magnitudes 5.5–7.8 earthquakes. Afterward, the values of stiffness and damping at the effective shear strain are determined from damping and shear modulus reduction curves. The process is iterated until the difference of damping and stiffness values in two consecutive iterations reaches less than a set of acceptable values (Kramer 1996). The following four inputs are required for ground response analysis : (1) Soil classification (on the basis of soil type, density, thickness and N value/shear-wave velocity), (2) depth to the base rock/EBL, (3) strong motion at base rock/EBL, and (4) damping and shear modulus with shear strain curves. The ground response analysis is done on SHAKE 2000 (Ordonez 2012). The SHAKE 2000 can convert the supplied outcrop strong motion to base rock motion before ground response analysis with its inbuilt capability by supplying the option at the beginning itself. The ground response analysis has been conducted for both far-field earthquake scenarios and near-field earthquake scenarios.

The damping ratio (β) and modulus reduction (G/G_{max}) versus shear strain curves of Schnabel (1973), Sun et al. (1988) and Seed and Idriss (1970) for rock, clay, and sand, respectively, which were used in the seismic microzonation study of nearby Gandhinagar region (Mohan et al. 2018) have been used in the present study to conduct ground response analysis. These curves are presented in Figs. 8 and 9. These curves are provided in the SHAKE database and used during calculations by selecting the options.

Table 6 The selected model parameters for simulation of SGM due to far-field ground earthquake scenarios

Magnitude (Mw)	7.0, 7.6 and 7.8
Fault length and width	(44 km and 18 km)*, (75 km and 35 km) ⁺ , (127 km and 39 km)*
Strike and dip	78° and 58° Yagi and Kikuchi (2001)
Slip distribution	Random
Shear wave velocity	3.6 km/s
Density	2.8 gm/cm ³
Stress drop	140, 160 and 180 bars
kappa	0.02, 0.025 and 0.03 Mandal et al. (2005)
Anelastic attenuation q(f)	508f ^{0.48} , 800f ^{0.42} , 790f ^{0.22} Singh et al. (1999), Singh et al. (2004) and Bodin et al. (2004)
Geometric spreading	1/R (R ≤ 40 km) Bodin et al. (2004) 1/R ^{0.5} (40 ≤ R ≤ 80 km) 1/R ^{0.55} (R ≥ 80 km)
Duration properties	f _c ⁻¹ (R < 10 km) Eastern North America f _c ⁻¹ + 0.16R (10 ≤ R ≤ 70 km) Atkinson and Boore (1995) f _c ⁻¹ - 0.03 (70 < R ≤ 130 km) f _c ⁻¹ + 0.04R (130 < R < 1000 km)
Pulsing percent	50%

*Wells and Coppersmith (1994)

⁺Yagi and Kikuchi (2001)**Table 7** Frequency dependent amplification generated for the Vs30 of 520 m/s (Boore and Joyner 1997)

Frequency (Hz)	Amplification
0.01	1
0.09	1.21
0.16	1.32
0.51	1.59
0.84	1.77
1.25	1.96
2.26	2.25
3.17	2.42
6.05	2.7
16.6	3.25
61.2	4.15

The ground response analysis is conducted for all parametric combinations of both earthquake scenarios and the surface strong motion is generated.

The PGA values at EBL, as well as the surface level of all the 20 boreholes, have been computed from the surface strong motion. The estimated mean PGA values due to all near-field earthquake scenarios at each borehole at a surface level have been given in Table 8 and

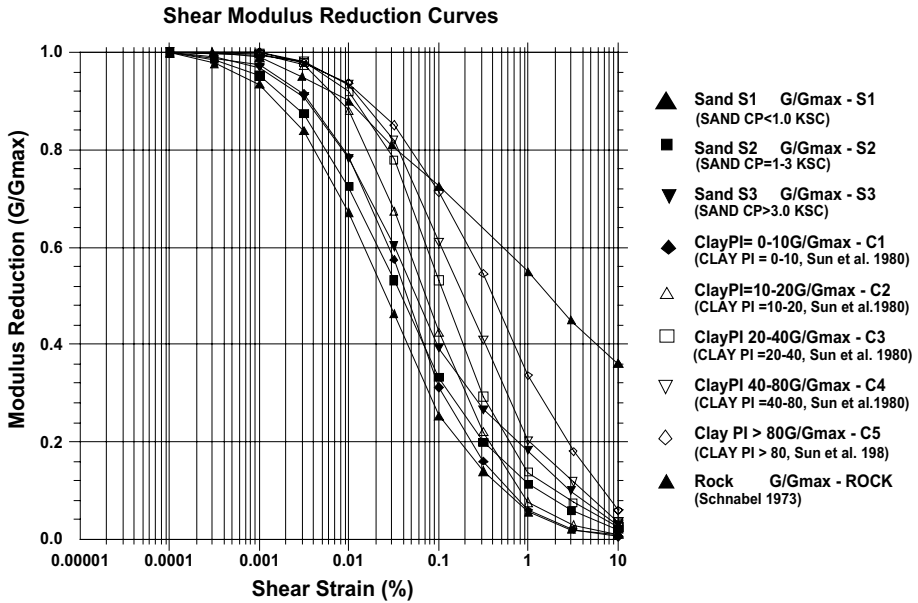


Fig. 8 The Modulus reduction versus shear strain curves used in the analysis for various soil types

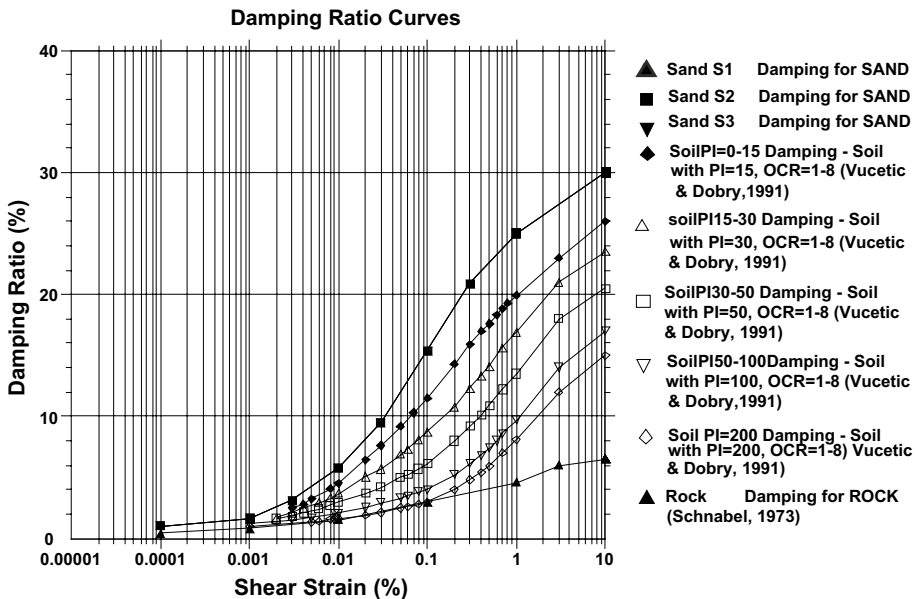


Fig. 9 The Damping ratio versus shear strain curves used in the analysis for various soil types

due to far-field earthquake scenarios in Table 9. The PGA distribution map for surface level due to near-field earthquake scenarios has been given in Fig. 10. The Bureau of Indian Standard [IS 1893 (Part 1)] has proposed the conversion factor from 5% damping to other dampings

Table 8 The borehole-wise mean PGA values (at surface) and amplification due to near-field scenario earthquake

Borehole no.	Mean base PGA (within) (cm/s ²)	Mean surface PGA (cm/s ²)	PGA amplification	Borehole no.	Mean base PGA (within) (cm/s ²)	Mean surface PGA (cm/s ²)	PGA amplification
BH-01	84.6	278.9	3.3	BH-11	88.9	234.2	2.6
BH-02	100.6	231.8	2.3	BH-12	53.5	126.2	2.4
BH-03	75	124.6	1.7	BH-13	67.9	154.3	2.3
BH-04	58.1	138	2.4	BH-14	77.4	184.8	2.4
BH-05	52.4	100.7	1.9	BH-15	74.8	194.5	2.6
BH-06	55.3	148.7	2.7	BH-16	64.8	111.8	1.7
BH-07	92	231.8	2.5	BH-17	67.4	213	3.2
BH-08	85.5	223.2	2.6	BH-18	57.8	138.4	2.4
BH-09	70.7	160.2	2.3	BH-19	83.6	192.6	2.3
BH-10	111.4	262.9	2.4	BH-20	53	114.4	2.2

Table 9 The borehole-wise mean PGA values (at surface) and amplification due to far-field earthquake

BH. no.	PGA at the base (cm/s ²)	Mean PGA at surface (cm/s ²)	PGA amplification	BH. no.	PGA at base (cm/s ²)	Mean PGA at surface (cm/s ²)	PGA amplification
BH-01	107.8	161.5	3.0	BH-11	107.8	143.4	2.7
BH-02	107.8	123.5	2.3	BH-12	107.8	138.2	2.6
BH-03	107.8	118.4	2.2	BH-13	107.8	139.9	2.6
BH-04	107.8	135.4	2.5	BH-14	107.8	135.2	2.5
BH-05	107.8	128.1	2.4	BH-15	107.8	154.6	2.9
BH-06	107.8	142.0	2.6	BH-16	107.8	125.6	2.3
BH-07	107.8	138.9	2.6	BH-17	107.8	142.3	2.6
BH-08	107.8	133.4	2.5	BH-18	107.8	125.1	2.3
BH-09	107.8	126.4	2.3	BH-19	107.8	141.4	2.6
BH-10	107.8	134.3	2.5	BH-20	107.8	133.9	2.5

based on material type, therefore the response spectra are calculated on the surface of every borehole for damping of 5%. In the case of a near-field earthquake, a total of 108 response spectra are generated at each borehole considering different parametric combinations. The mean, mean+standard deviation (SD) and mean-SD response spectra are also estimated at each borehole. All response spectra computed due to near-field earthquake scenarios at each borehole have been shown in Fig. 11. The spectral acceleration maps at different periods (0.2 s, 0.55 s, 1.0 s and 1.25 s) have also been prepared given in Fig. 12. The amplification of ground motion between EBL and surface levels due to near-field earthquake scenarios has been given in Fig 13. In the case of far-field earthquake scenarios. The PGA distribution map for surface level due to far-field earthquake scenarios has been given in Fig. 14. In the case of a far-field earthquake, a total of 81 response spectra are generated at each borehole considering different parametric combinations. The mean, mean+standard deviation (SD) and mean-SD response spectra are also estimated at each borehole. All response spectra computed due to

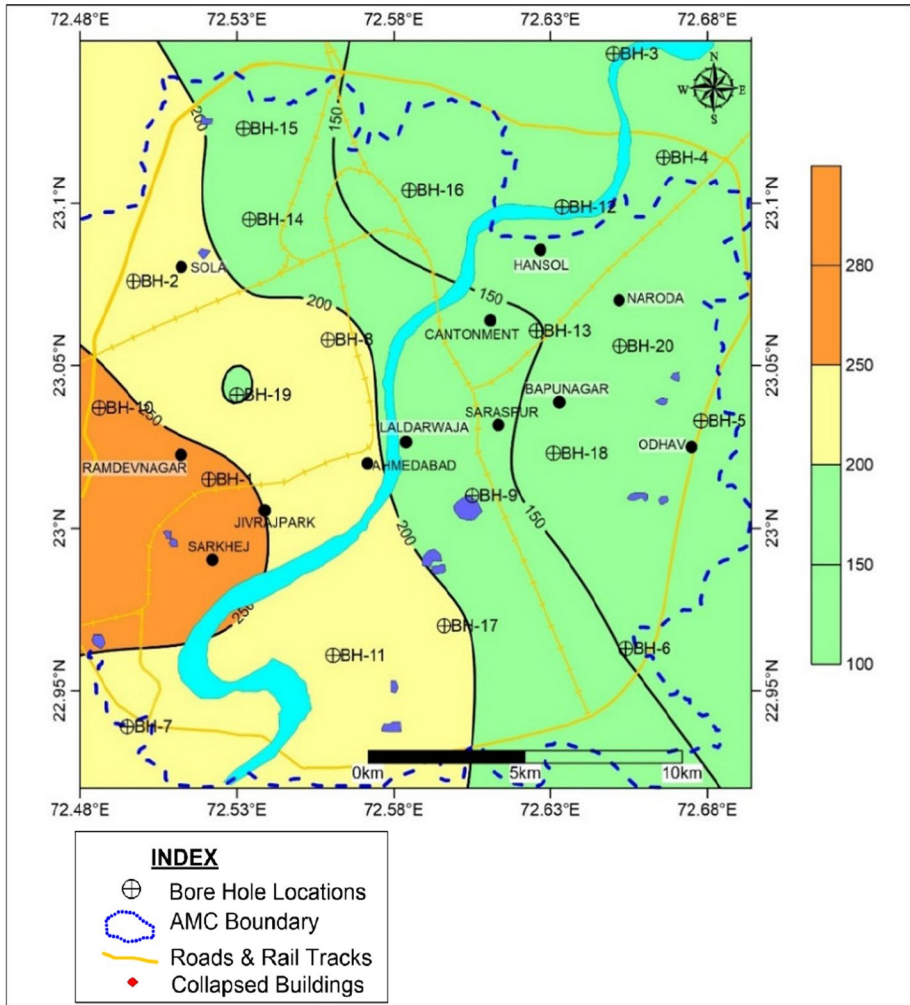


Fig. 10 The surface peak ground acceleration distribution map of Ahmedabad city area for near-field earthquake scenario prepared using SHAKE program

far-field earthquake scenarios at each borehole have been shown in Fig. 15. The spectral acceleration values at each borehole at the surface level have also been extracted from the response spectra and the spectral acceleration distribution maps have been prepared for periods of 0.2 s, 0.55 s, 1.0 s and 1.25 s. The spectral acceleration (SA) distribution maps for far-field earthquake scenarios have been shown in Fig. 16. The amplification of ground motion between EBL and surface levels due to far-field earthquake scenarios has been given in Fig. 17.

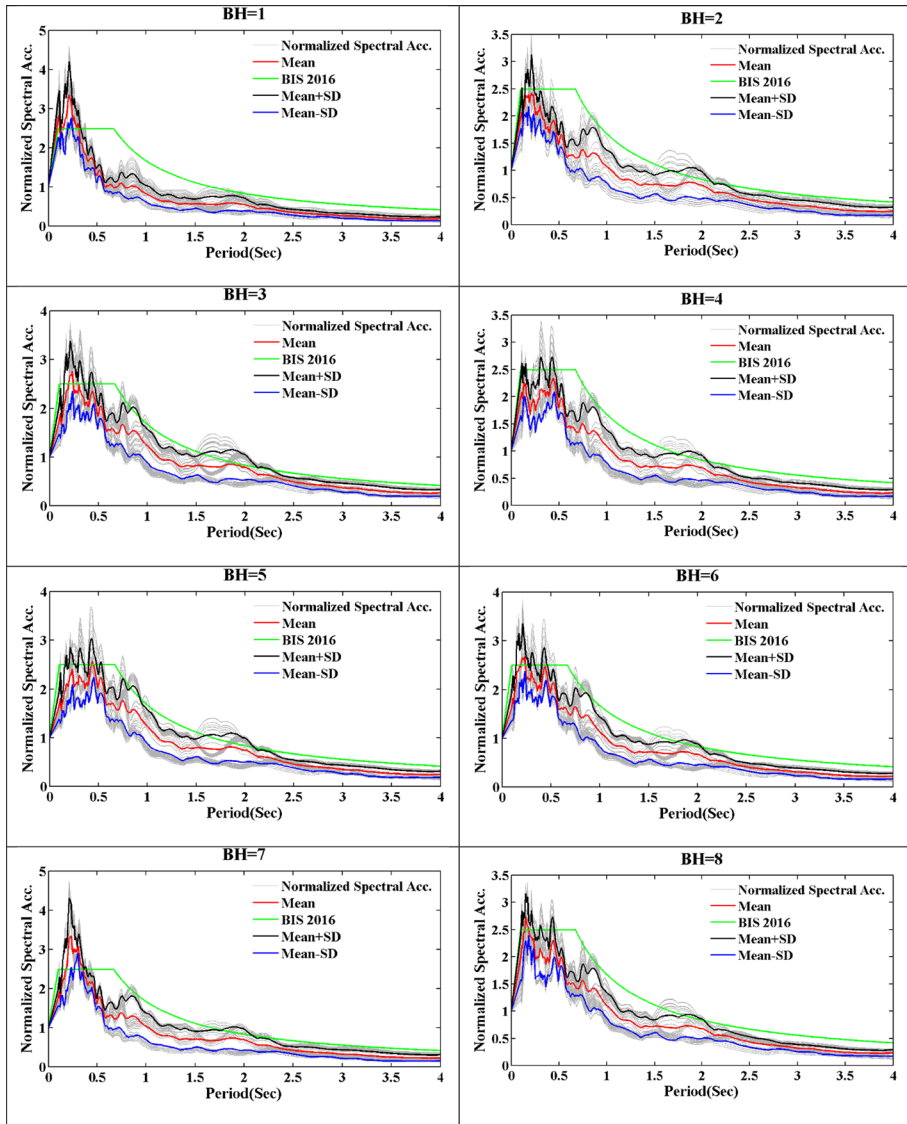


Fig. 11 Borehole-wise normalized spectral acceleration plots with Mean and Standard Deviation for Near-Field earthquake consideration

4 Results and discussion

The ground response analysis is conducted using soil models prepared from 20 boreholes of the Ahmedabad city (Fig. 4). The EBL has been established between 24 and 54 m (Table 1 and Fig. 7). The input strong motion (at EBL) when passing within the soil layers (present above EBL) during ground response analysis, either gets amplified or attenuated

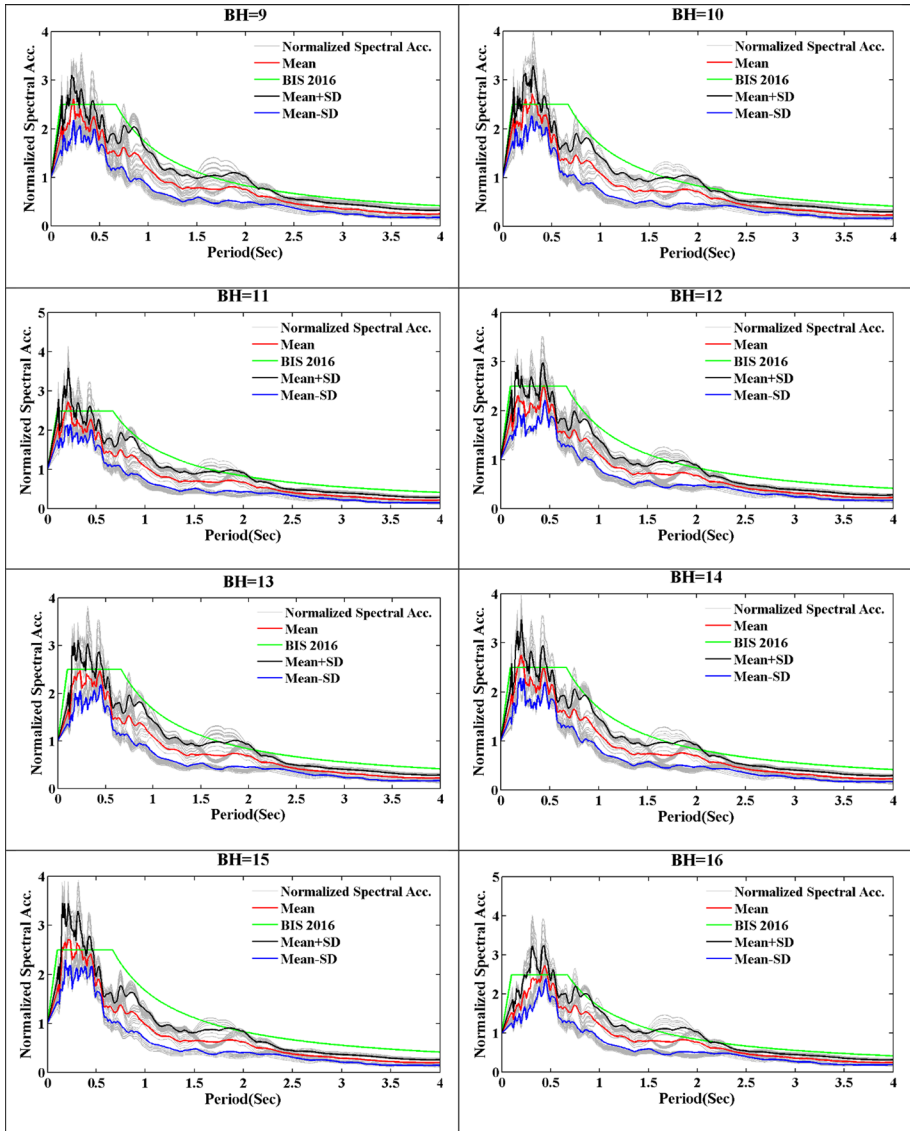


Fig. 11 (continued)

on the boundaries of every soil layer. Finally, the resultant strong motion is obtained at the surface.

The strong motion for near-field earthquake scenarios (Mw 5.5, 6.0 and 6.5) along ECF and WCF are generated using the Stochastic finite fault modeling technique. To reduce uncertainty in parameters, a suite of parameter based on past studies in the region are used. A total of 108 parametric combinations (2 faults (ECF and WCF), three magnitudes, two quality factors, three stress drops (Table 5) are used for the estimation of strong motion at EBL due to near-field earthquake scenarios. The ground motion of each of the 108

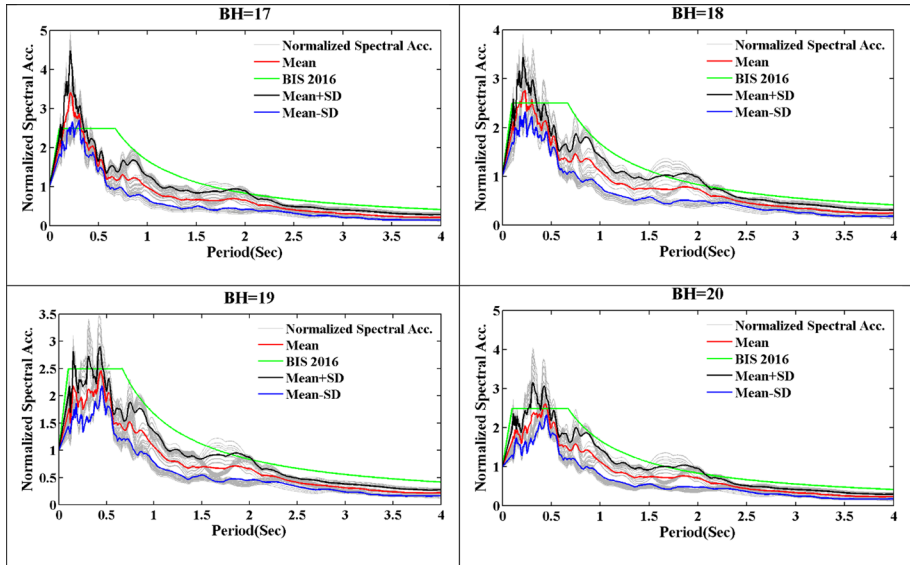


Fig. 11 (continued)

input parametric combinations for the near-field earthquake scenarios with PGA varying between 52.4 and 111.4 cm/s^2 is applied at EBL. The mean surface PGA is thus estimated from 100.7 to 278.9 cm/s^2 . The PGA is found high in western Ahmedabad in comparison to eastern Ahmedabad due to low shear wave velocity (Fig. 6) and the presence of clay with medium plasticity (Fig. 5b). The maximum PGA (of 278.9 cm/s^2) has been estimated in the west-central part of Ahmedabad at BH-1. The PGA distribution at the surface is given in Fig. 10 and Table 8. The response spectra (on 5% damping) at the surface level of each borehole and the mean normalized response spectra at each borehole are given in Fig. 11. The natural frequencies of buildings depend on two main parameters (mass and stiffness) which are related as: $f = 1/2\pi \sqrt{(K/M)}$; K is stiffness and M is the mass of the building. Therefore, taller buildings tend to be more flexible and have low natural frequencies in comparison to shorter buildings. In general, the building with 0.2 s corresponds to a natural period of 1–2 story building, 0.55 s for 4–5 story building, 1 s high rise building and 1.25 s for large story building. Therefore, the mean SA distribution maps for 0.2 s, 0.55 s, 1 s and 1.25 s period (large story building) are prepared at the surface level and are shown in Fig. 12. The mean PGA amplification factor is also calculated at all the boreholes. It is varying from 1.6 to 3.3 (Fig. 13 and Table 8). The maximum amplification is observed at boreholes BH-01 and BH-17 due to low shear wave velocity (Fig. 6) and the presence of clay with medium plasticity (Fig. 5 b). Moreover, the stiffness contrast between the layers also creates the amplification factor. The presence of a 6 m clay layer followed by sand at borehole BH-01 also suggested an abrupt increase in ground motion/amplification.

The response spectra of all the boreholes are computed at 5% damping from 0.1 to 4.0 s. The maximum mean SA of 680 cm/s^2 (70% more than BIS suggested values National code) is observed at 0.2 s (Fig. 12a) (corresponds to 1–2 story buildings), in the western part of the Ahmedabad city area around borehole BH-01 (comprising of the clayey top layer with low shear wave velocity). The mean SA is found in the range of 600–650 cm/s^2 near BH-7 and BH-11 (in the south-western part). At the period of 0.55 s (analogous to the natural

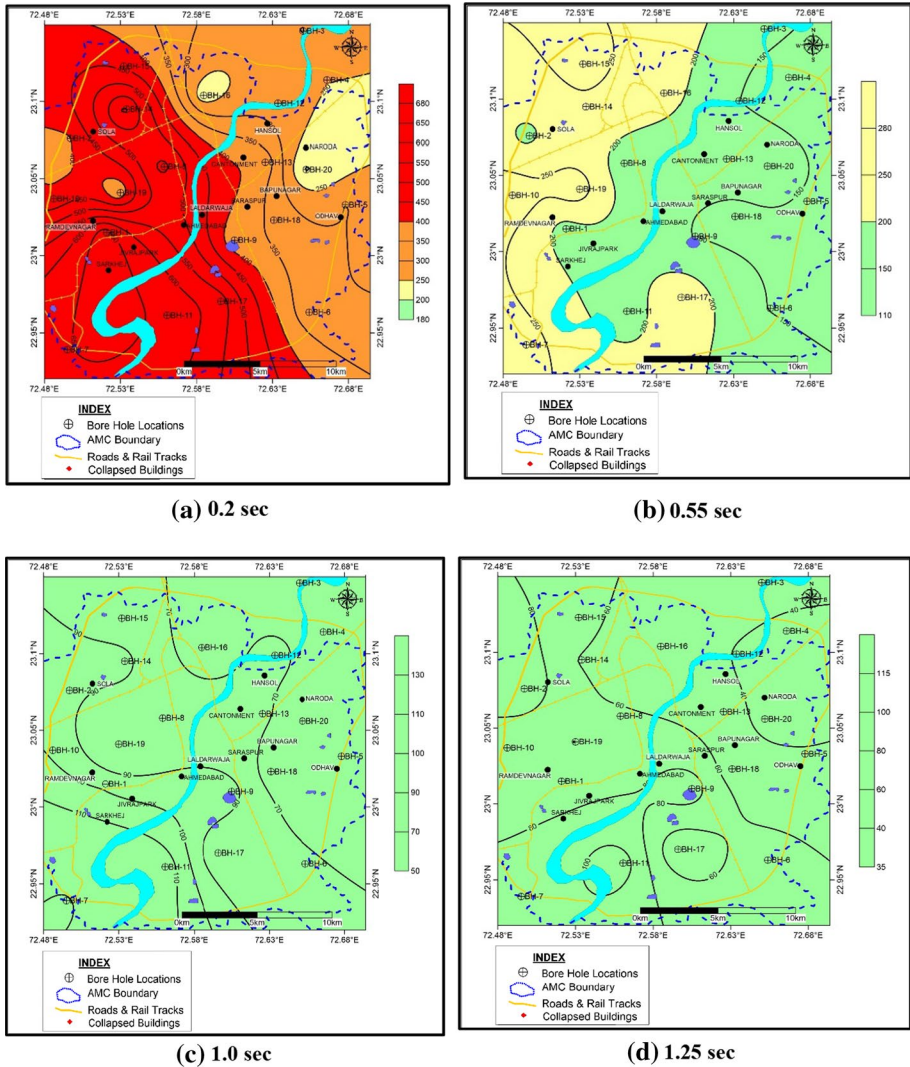


Fig. 12 The spectral acceleration distribution maps of the Ahmedabad City for near-field earthquake scenario

period of 5–6 story buildings) higher SA is observed in the north-western, west-central and southern parts of the Ahmedabad city. The near-field earthquakes generate low energy at high periods/low frequencies, the maximum mean SA of 280 cm/s² is calculated (28% less than National code) at BH-10 and BH-19 in the west-central part of the Ahmedabad city (Fig. 12b). The maximum mean SA of 130 cm/s² (50% less than the National code) at BH-07 is computed in the south-western part of the Ahmedabad city at 1.0 s (corresponding to the natural period of 10 story buildings) (Fig. 12c). The maximum SA of 115 cm/s² (less than 50% of the National code) at BH-11, is computed in the south-western part of the

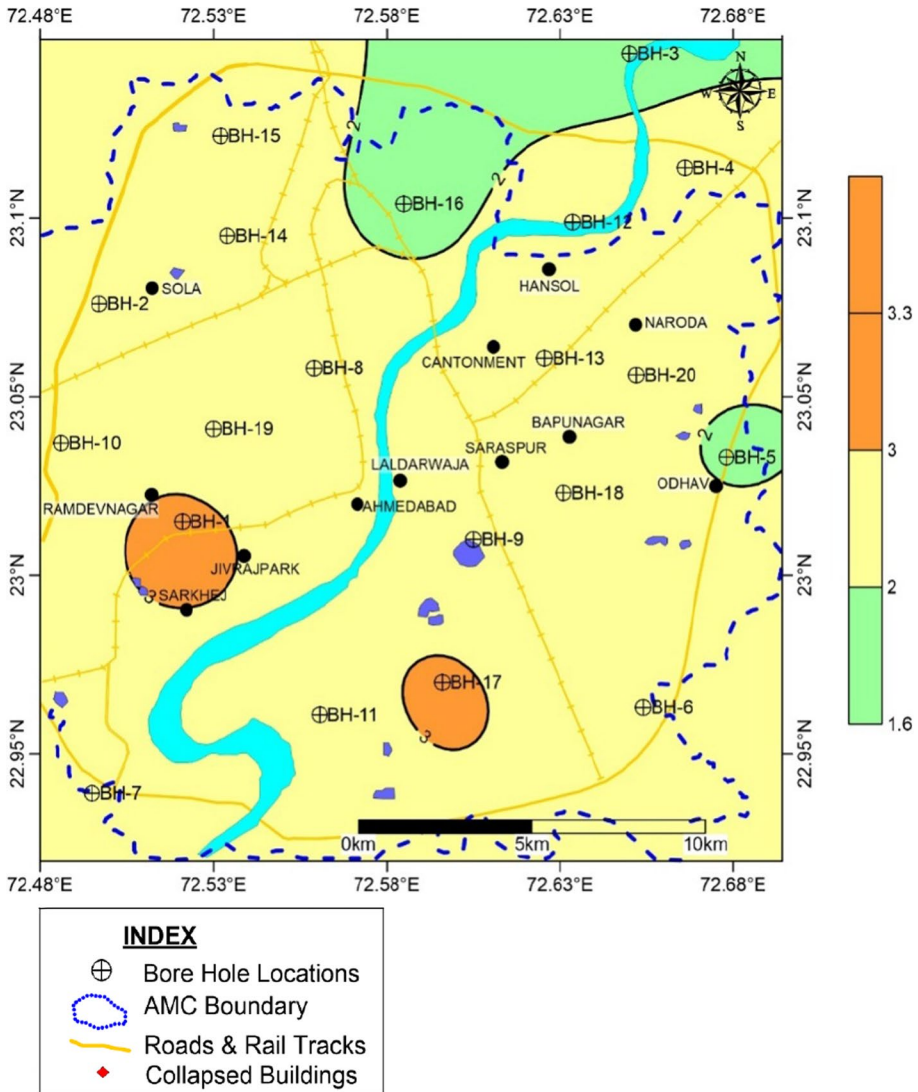


Fig. 13 Mean Amplification due to near-field earthquake scenario

Ahmedabad city at 1.25 s (corresponding to the natural period of 12–15 story buildings) (Fig. 12d).

In the case of far-field earthquake scenarios, the input motion with a mean PGA (estimated from 81 input parametric combinations) of 107.8 cm/s² is applied at EBL. The PGA at the surface level has been computed through ground response analysis. The computed mean surface PGA is found to vary from 118.4 to 161.5 cm/s² (Table 9). The highest mean PGA of 161.5 cm/s² is observed in the west-central portion and the lowest PGA of 118.4 cm/s² is estimated in the north-eastern part of Ahmedabad. The maximum mean PGA (161.5 cm/s²) is observed at BH-01 (comprising of clay with medium plasticity and

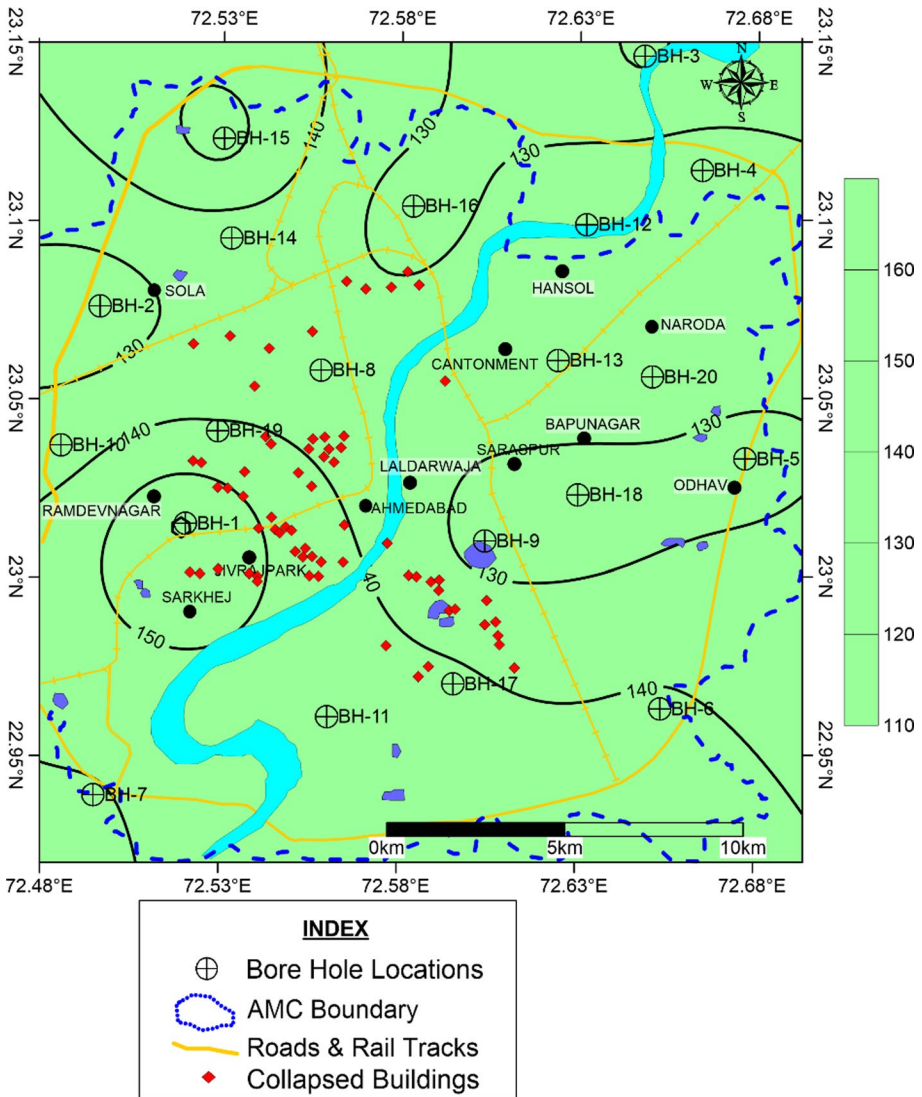


Fig. 14 The surface peak ground acceleration (in cm/s²) distribution map of Ahmedabad City for a far-field earthquake with the location of damaged buildings

low V_s values) and the minimum at BH-03 (comprising of sand with high density and higher V_s in the top layer). The mean PGA amplification factor is also calculated at all boreholes and is found to vary from 2.2 to 3.0 (Table 9), with maximum amplification at BH-01.

The mean response spectra are determined at all the boreholes at 5% damping from 0.1 to 4.0 s (Fig. 15). The SA maps at different periods (0.2, 0.55, 1.0 and 1.25 s) are prepared (Fig. 16). At 0.2 s (corresponding to 2–3 story buildings) (Fig. 16a), the maximum mean SA of 500 cm/s² is observed (~ 28% more than the National code) in the

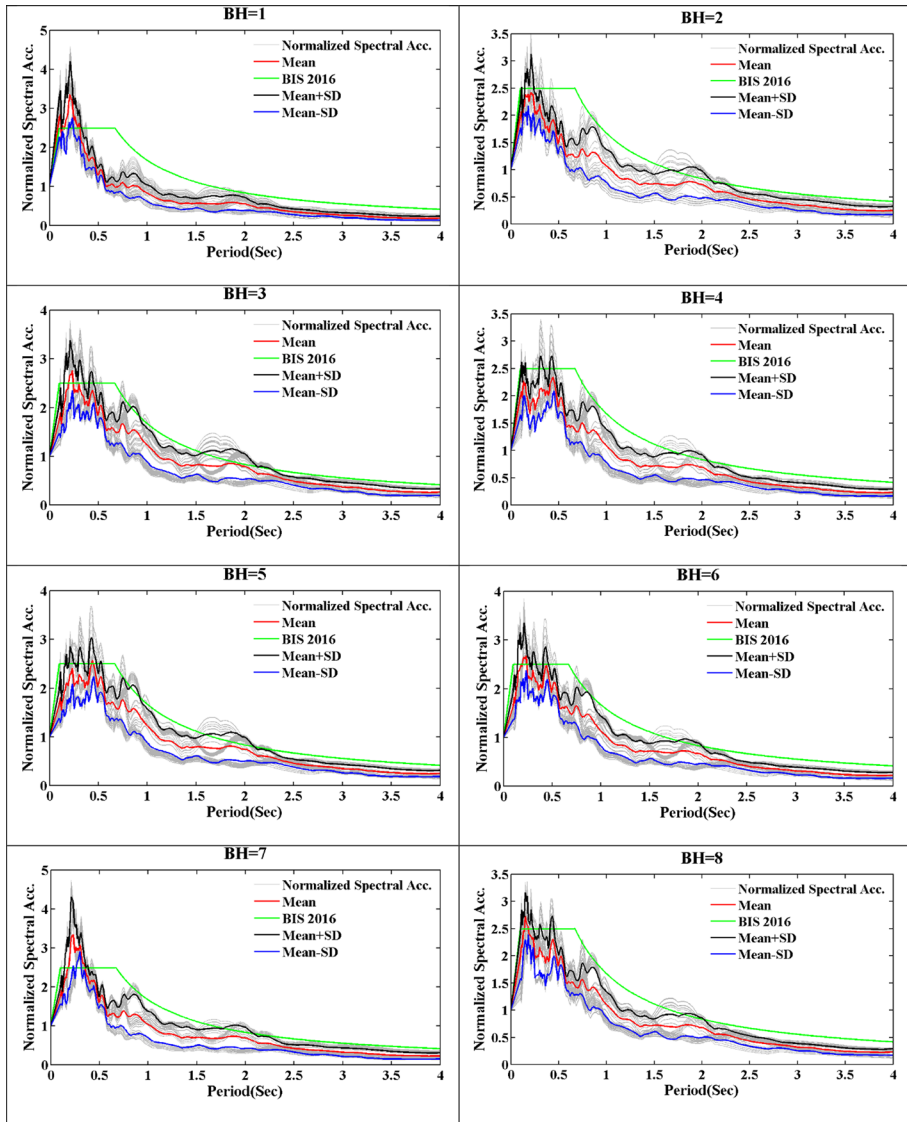


Fig. 15 Borehole-wise normalized response spectra plots with Mean and Standard Deviation for Far-Field earthquake consideration

west-central part of Ahmedabad city at BH-01. At periods 0.55 s (corresponding to 5–6 story buildings), the maximum mean SA of $\sim 270 \text{ cm/s}^2$ (31% less than the national code) is computed in the southeastern part of the city at BH-06 (Fig. 16b). At periods 1.0 and 1.25 s, the highest mean SA of 110 cm/s^2 and 100 cm/s^2 ($\sim 60\%$ less than the national code), respectively are observed in the southeastern part (at BH-06) and north-western part (at BH-14) of the city (Fig. 16c, d) and lowest in the west-central part of the city (at BH-02).

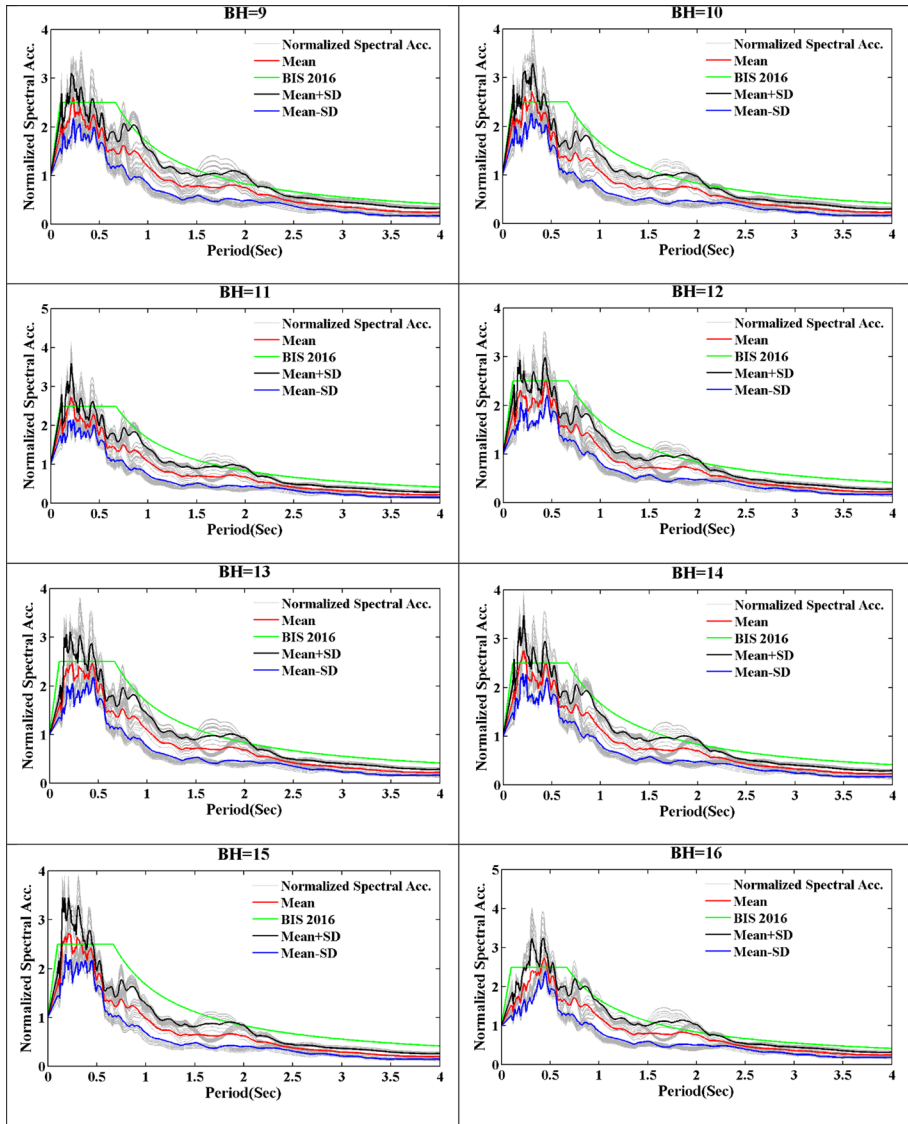


Fig. 15 (continued)

The national disaster management authority (NDMA) has proposed the probabilistic seismic hazard assessment map of India at A-type soil class (V_{s30} of 1500 m/s) (NDMA 2010) and suggested a PGA value of $\sim 140 \text{ cm/s}^2$ in Ahmedabad at 2% probability of exceedance (2% PE) in 50 years. Parvez et al. (2003) have conducted the deterministic seismic hazard assessment of India based on the Modal Summation technique of Costa et al. (1993) and suggested the design ground acceleration of $\sim 150\text{--}300 \text{ cm/s}^2$ in Ahmedabad city at the surface level. Chopra et al. (2012b, a) have conducted the deterministic seismic hazard assessment of Gujarat considering far-field

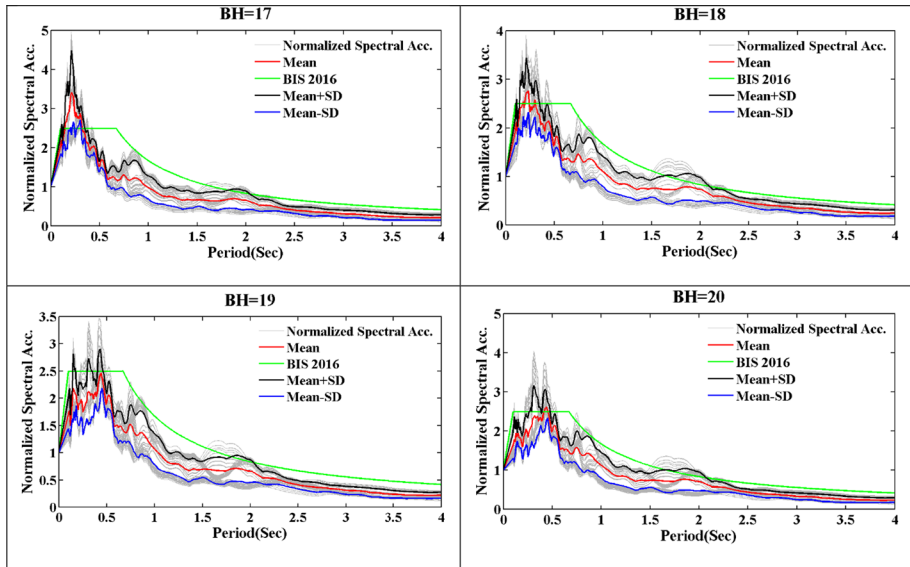


Fig. 15 (continued)

earthquake using Stochastic finite fault modeling technique and suggested the PGA of 41 cm/s^2 at the surface level. Rao et al. (2012) have conducted the classical deterministic seismic hazard assessment of Ahmedabad city and suggested the PGA in the range of $140\text{--}440 \text{ cm/s}^2$ at rock level. Trivedi (2011) has conducted the de-convolution analysis considering Far-field earthquake considering single accelerogram of 2001 Bhuj earthquake recorded at the passport office building of Ahmedabad and suggested the PGA of the order of $96\text{--}194 \text{ cm/s}^2$ that matches with the PGA estimated through far-field earthquake scenarios in the present study ($100\text{--}162 \text{ cm/s}^2$). The results of the present study match well with the regional study of Parvez (2003) and the study carried out by NDMA (2010), after incorporation of soil effects (amplification from A to D type soil class).

Ahmedabad has already experienced damages due to two large earthquakes in the past (1819-ABEQ and 2001-BEQ). The shaking minarets of the Jama Masjid located in the central part of Ahmedabad (near Lal Darwaja area) (Fig. 12) were damaged due to the 1819-ABEQ. The current investigation has also suggested the high PGA in the range of $\sim 135 \text{ cm/s}^2$ at the Jama Masjid site due to the far-field earthquake scenarios, which is analogous to 1819 or 2001 earthquakes (Fig. 14). In Ahmedabad, 80 buildings of 1021 flats and 82 other houses had collapsed during the 2001 Bhuj Eq. (Mishra 2004) mainly in the west-central part [in the vicinity of BH-01, BH-17, and BH-19 (Fig. 14)] of Ahmedabad city. In the present investigation, the maximum PGA values of $135\text{--}150 \text{ cm/s}^2$ are also estimated in the west-central part (Fig. 14).

Most of the collapsed buildings were close to BH-01 and BH-19 where clay is present at/near-surface, with a very low N-value, low shear wave velocity and medium plasticity. The clay with interbeds of silty sand is present in the subsurface. In the Loma Prieta earthquake ($M_s 7.1$) that occurred on October 17, 1989, the maximum (up to 80%) loss of lives occurred about 50 miles away (at Treasure Island) from the fault

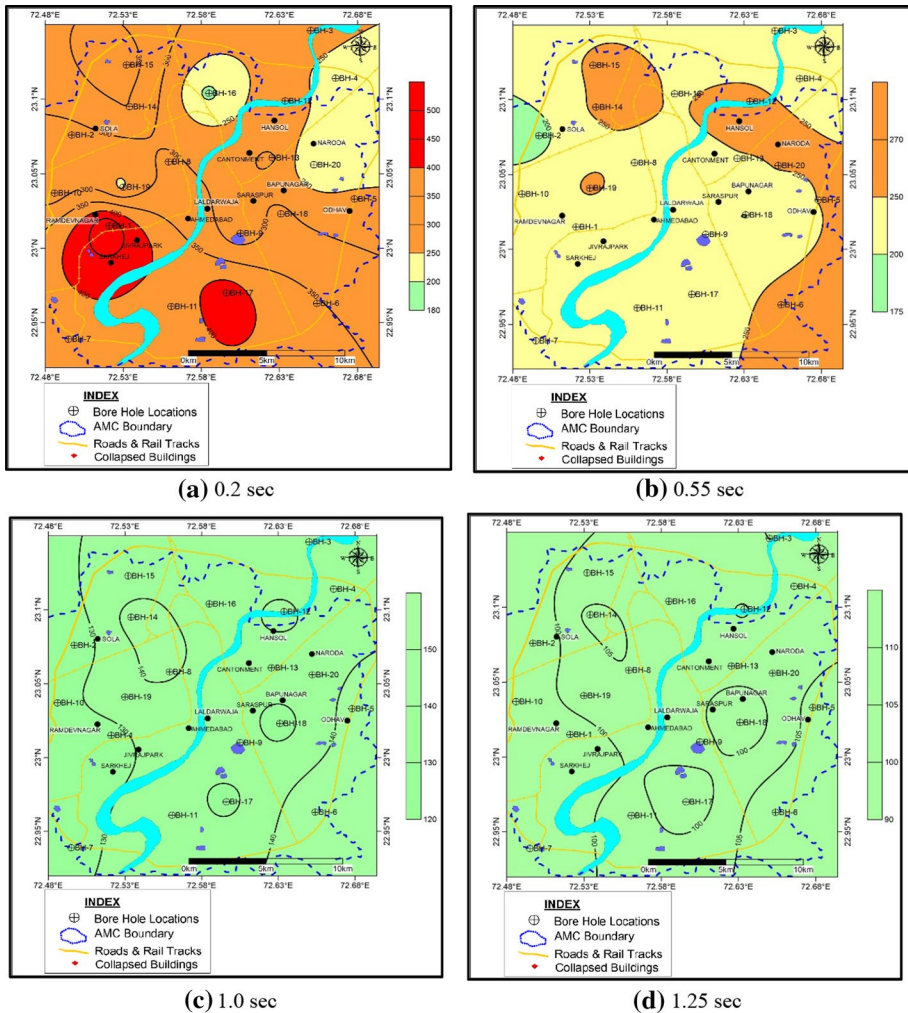


Fig. 16 The spectral acceleration distribution maps of the Ahmedabad city area for far-field earthquake scenario at: **a** 0.2 s, **b** 0.55 s, **c** 1.0 s, and **d** 1.25 s

rupture zone. Ferritto et al. (1993) from Naval Civil Engineering Lab, California have conducted the ground response analysis at Treasure Island, which is a naval base. The soil of Treasure Island consists of bay mud deposits, a high plasticity silty clay (Ferritto et al. 1993). The study concluded that high plasticity clay deposits can be a possible source of ground motion amplification. The Clay with medium plasticity found at BH-01 and BH-19 (in the western central area of Ahmedabad) might be one of the causes of devastation.

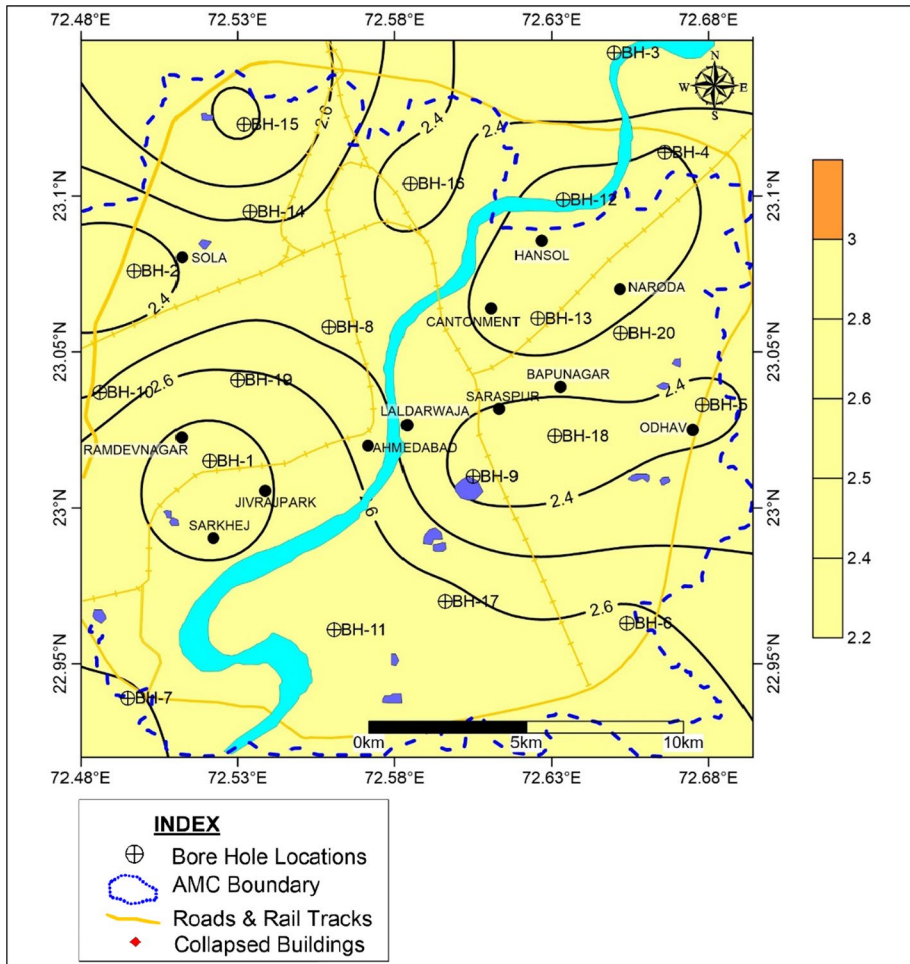


Fig 17 Mean Amplification due to far-field earthquake scenario

5 Conclusion

The micro-level seismic hazard assessment is carried out at Ahmedabad city through characterization of near-surface using seismological, geotechnical and geophysical investigations. The ground response analysis is carried out at 20 boreholes varying in depths from 40 and 80 m. The study highlighted the following points:

- (1) In Ahmedabad city, 3–18 m thick clay (from the surface) is found west of the Sabarmati River and sand layer with a thickness of 2–31 m is found in the eastern part of the city, east of Sabarmati River (except SE part, where clay thickness ~ 15 m is present).
- (2) The mean surface PGA of the order of 101–279 cm/s^2 (maximum PGA, 70% higher than the national code) is computed for the near-field earthquake scenarios and 118–162 cm/s^2 due to far-field earthquake scenarios.

- (3) Comparatively higher PGA is computed in the western portion of the Ahmedabad city (due to near-field earthquake scenarios) than the eastern portion. The highest PGA of 279 cm/s^2 is found in the west-central part of the Ahmedabad city due to near-field earthquake scenarios. The highest mean PGA of 162 cm/s^2 is observed in the west-central portion of the city due to far-field earthquake scenarios. The damage during the 1819 Allah Bund and 2001 Bhuj earthquakes have occurred in the west-central part of the city.
- (4) In the case of near-field earthquake scenarios, the mean SA is found to be 70% more than the National code for 0.2–0.3 s (2–3 story buildings), ~ 30% less for 0.55 s (5–7 story buildings) and ~ 50% less for 1–1.25 s (10–15 story high rise buildings). For far-field earthquake scenario, the SA is found to be 28% more than the National code for 0.2–0.3 s (2–3 story buildings), ~ 31% less for 0.55 s (5–7 story buildings) and ~ 40% less for 1–1.25 s (10–15 story high rise buildings).
- (5) The amplification factor of 1.6–3.3 is found from both earthquake scenarios in the Ahmedabad region.

Acknowledgements Authors are thankful to Director General, Institute of Seismological Research for permitting to publish this research work and to the Ministry of Earth Sciences (MoES) to provide funds for the Seismic Microzonation study of the Ahmedabad city, Gujarat (India) under grant MOES/P.O. (Seismo)/1(41)/2009.

References

- Aki K (1966) Generation and propagation of G waves from the Niigata earthquake of June 14, 1964. Part 2: Estimation of earthquake moment, released energy and stress-strain drop from G wave spectrum. *Earthquake Research Institute, University of Tokyo*, vol 44, pp 73–88
- Aki K (1967) Scaling law of seismic spectrum. *J Geophys Res* 72:1217–1231
- Anbazhagan P, Sitharam TG (2008) Seismic microzonation of Bangalore. *J Earth Syst Sci* 117(S2):833–52
- Anderson JG, Hough SE (1984) A model for the shape of the Fourier amplitude spectrum of acceleration at high frequencies. *Bull Seismol Soc Am* 74(1):969–1993
- Atkinson GM, Boore DM (1995) Ground motion relations for eastern North America. *Bull Seismol Soc Am* 85:17–30
- Beresnev IA, Atkinson GM (1998a) Stochastic finite-fault modeling of ground motions from the 1994 Northridge, California, earthquake. I. Validation on rock sites. *Bull Seismol Soc Am* 88:1392–1401
- Beresnev IA, Atkinson GM, (1998b) FINSIM—a FORTRAN program for simulating stochastic acceleration time histories from finite faults. *Seismol Res Lett* 69:27–32
- Bhandari T, Thaker TP, Rao KS (2013) Seismic hazard analysis of Ahmedabad City. In: *Proceedings of Indian geotechnical conference December 22–24, 2013, Roorkee*, pp 1–8
- BIS (2016) IS 1893: Part 1: 2016: Criteria for earthquake resistant design of structures—Part 1: General provisions and buildings, Bureau of Indian standard
- Biswas SK (1982) Rift basins in western margin of India and their hydrocarbon prospects with special reference to Kutch Basin. *J Ame Assoc Petrol Geol* 10:1497–1513
- Biswas SK (1987) Regional tectonic framework, structure and evolution of western marginal basins of India. *Tectonophysics* 135:307–327
- Biswas SK, Bhasin AL, Ram J (1994) Classification of sedimentary basins of India in the framework of plate tectonics. In: *Proc. Second Symp. Petroliferous basins of India, KDMIPE, Dehradun*, vol 1, pp 1–42
- Biswas SK (1999) A review on the evolution of rift basins in India during Gondwana with special reference to western Indian basins and their hydrocarbon prospects. *Proc Indian Natl Sci Acad* 65:261–283
- Bodin P, Horton S (2004) Source parameters and tectonic implications of aftershocks of the Mw 7.6 Bhuj Earthquake. *Bull Seismol Soc Am* 94:1658–1669
- Bodin P, Malagnini L, Akinci A (2004) Ground-motion scaling in the kachchh basin, India, deduced from aftershocks of the 2001 M_w 7.6 Bhuj earthquake. *Bull Seismol Soc Am* 94:1658–1669

- Boore DM, Joyner WB (1997) Site amplification for generic rock sites. *Bull Seismol Soc Am* 87(2):327–341
- Chandler AM, Lam NTK, Tsang HH (2006) Near-surface attenuation modelling based on rock shear-wave velocity profile. *Soil Dyn Earthq Eng* 26:1004–1014
- Chopra S, Kumar D, Rastogi BK (2010) Attenuation of high-frequency P and S waves in the Gujarat Region, India. *PAGEOPH*. <https://doi.org/10.1007/s00024-010-0143-8>
- Chopra S, Kumar D, Rastogi BK, Choudhary P, Yadav RBS (2012) Deterministic seismic scenario in Gujarat, India. *Nat Hazards* 60:1157–117
- Chopra S, Kumar V, Suthar A, Kumar P (2012) Modeling of strong motions for 1991 Uttarkashi, 1999 Chamoli earthquakes, and a hypothetical great earthquake in Garhwal-Kumaun Himalaya. *Nat Hazards* 64(2):1141–1159
- Chen C-T, Chang S-C, Wen K-L (2017) Stochastic ground motion simulation of the 2016 Meinong, Taiwan earthquake. *PI Space* 69:62. <https://doi.org/10.1186/s40623-017-0645-z>
- Costa G, Panza GF, Suhadolc P, Vaccari F (1993) Zoning of the Italian territory in terms of expected peak ground acceleration derived from complete synthetic seismograms. *J Appl Geophys* 30:149–160. [https://doi.org/10.1016/0926-9851\(93\)90023-R](https://doi.org/10.1016/0926-9851(93)90023-R)
- Danda N, Rao CK, Kumar A (2017) Geoelectric structure of northern Cambay rift basin from magnetotelluric data. *Earth PI Space* 69:140
- Dixit MM, Tewari HC, Rao CV (2010) Two-dimensional velocity model of crust beneath the South Cambay Basin, India from refraction and wide-angle reflection data. *Geophys J Int* 181:635–652
- Ferritto JM (1993) Effects on high plasticity clay deposits on site ground amplification. In: the Proceeding Third international conference on case histories in Geotechnical Engineering, St. Louis, Missouri, 1–4 Jun 1993, paper No. 3.33 pp. 1521-1527 (<https://scholarsmine.mst.edu/icchge/3icchge/3icchge-session03/19>)
- Ganpathy GP (2011) First level seismic microzonation map of Chennai city- a GIS approach. *Nat Hazards Earth Syst Sci* 11(2):549–559
- Gupta A, Sutar AK, Chopra S, Kumar S, Rastogi BK (2012) Attenuation characteristics of coda waves in Mainland Gujarat (India). *Tectonophysics* 530–531:264–271
- Hartzell SH (1978) Earthquake aftershocks as green functions. *Geophys Res Lett* 5:1–4
- Irikura K (1983) Semi empirical estimation of strong ground motion during large earthquakes. *Bull Dis Prev Res Inst (Kyoto Univ.)* 33:63–104
- Irikura K (1992) The construction of large earthquake by a superposition of small events. In: Proceedings of the 10th world conference on earthquake engineering, vol 1, pp 727–730
- Irikura K, Kamae K (1994) Estimation of strong ground motion in broad frequency band based on a seismic source scaling model and an empirical Green's function technique. *Annali di Geo Fisica XXXVII*:1721–1743
- ISR (2013) Annual report of the institute of seismological research of the year 2012–13, pp. 256
- Iyenger RN, Raghukanth STG (2006) SGM estimation during the Kutch, India. *Earthq Pure Appl Geophys* 163:154–173
- Kaila KL, Tewari HC, Krishna VG, Dixit MM, Sarkar D, Reddy MS (1990) Deep seismic sounding studies in the north Cambay and Sanchar basins, India. *Geophys J Int* 103:621–637
- Kramer SL (1996) *Geotechnical earthquake engineering*. Prentice Hall, New Jersey, p 653
- Kumar S (2015) Source parameters, scaling relations and kappa model for small earthquakes in Kachchh and Saurashtra regions of Gujarat, India. Ph.D. thesis. Kuk. Uni. Kurukshetra. p 131
- Mandal P, Chadha RK, Satyarmury C, Raju P, Kumar N (2005) Estimation of site response in Kachchh, Gujarat, India, region using H/V spectral ratios of aftershocks of the 2001 M w 7.7 Bhuj Earthquake. *Pure Appl Geophys* 162:2479–2504
- Martin S, Szeliga W (2010) A catalog of felt intensity data for 570 earthquakes in India from 1636 to 2009. *Bull Seismol Soc Am* 100(2):562–569
- Mehr SS, Chamyal LS (1997) The quaternary geology of Gujarat alluvial plains. *Indian National Science Academy*, p 98
- Midorikawa S (1993) Semi empirical estimation of peak ground acceleration from large earthquakes. *Tectonophysics* 218:287–295
- Mishra PK (2004) The Kutch earthquake–2001: recollections, lessons, and insights. National Institute of Disaster Management, New Delhi
- Mohan K (2014) Seismic hazard assessment in the kachchh region of Gujarat (India) through deterministic modeling using a semi-empirical approach. *Seismol Res Lett* 85(1):117–125
- Mohan K, Kumar GP, Chaudhary P, Choudhary VK, Nagar M, Khushwaha D, Patel P, Gandhi D, Rastogi BK (2017) Magnetotelluric investigations to identify geothermal source zone near Chabsar hot-water spring site Ahmedabad, Gujarat, Northwest India. *Geotherm* 65(2017):198–209

- Mohan K, Rastogi BK, Pancholi V, Sairam B (2017) Estimation of strong motion parameters in the coastal region of Gujarat using geotechnical data, soil dynamics and earthquake engineering. *Soil Dyn Earthq Eng* 92:561–572
- Mohan K, Rastogi BK, Pancholi V, Gandhi D (2018) Seismic hazard assessment at micro level in Gandhinagar (the capital of Gujarat, India) considering soil effects. *Soil Dyn Earthq Eng* 109:354–370
- Motazedian D, Atkinson GM (2005) Stochastic finite-fault modeling based on dynamic corner frequency. *Bull Seismol Soc Am* 95:995–1010
- Motazedian D, Moinfar A (2006) Hybrid stochastic finite fault modeling of 2003, M6.5, Bam earthquake (Iran). *J Seismol* 10:91–103
- Nath SK, Thingbaijam KKS, Raj A (2008) Earthquake hazard in Northeast India—a seismic microzonation approach with typical case studies from Sikkim Himalaya and Guwahati city. *J Earth Syst Sci* 117(S2):809–831
- NDMA (2010) Development of probabilistic seismic hazard map of India, final technical report of the working committee of experts (WCE) constituted by the National Disaster Management Authority Govt. of India, New Delhi, p 80
- NEHRP (2003) NEHRP recommended provisions for seismic regulations for new buildings and other structures (FEMA 450), p 338
- Oldham T (1883) A catalogue of Indian earthquakes from the earliest time to the end of A.D. 1869. *Meml Geol Surv India* 19(3):163–215
- Ordonez Gustavo A (2012) SHAKE 2000- a compute program for the 1-D analysis of geotechnical earthquake engineering problems. GeoMotions, LLC, Lacey
- Parvez AI, Vaccari F, October GF (2003) A deterministic seismic hazard map of India and adjacent areas. *Geophys J Int* 155:489–508
- Peterson MD, Rastogi BK, Schweig GES, Harmsen SC, Gomberg JS (2004) Sensitivity analysis of seismic hazard for northwestern portion of the state of Gujarat, India. *Tectonics* 23:105–115
- Pomonis A, Coburn AW, Spence RJS (1993) Seismic vulnerability, mitigation of human casualties and guidelines for low-cost earthquake-resistant housing. STOP Disasters. Newsletter of the United Nations International Decade for natural disaster reduction no. 12
- Raghucharan MC, Somala SN (2017) Simulation of strong ground motion for the 25 April 2015 Nepal (Gorkha) Mw 7.8 earthquake using the SCEC broadband platform. *J Seismol* 21(4):777–808
- Rao NP (2014) Seismic microzonation of Jabalpur Urban Area. GSI Publication, Bengaluru
- Rao SK, Thaker TP, Aggarwal A, Bhandari T (2012) Deterministic seismic hazard analysis of Ahmedabad region, Gujarat. *Int J Earth Sci Eng* 5(2):206–213
- Rapolu N, Mandal P (2014) Source parameters of the 2001 Mw 7.7 Bhuj earthquake, Gujarat, India, after-shock sequence. *J Geol Soc India* 83(5):517–531
- Rastogi BK (2014) Seismicity and earthquake hazard studies in Gujarat. *J Earthq Sci Eng* 1:110–123
- Rastogi BK (2016) Seismicity of Indian stable continental region. *J Ind Soc Earthq Sci* 3:57–92
- Rastogi BK, Aggarwal SK, Rao N, Choudhury P (2012) Triggered/migrated seismicity due to the 2001 Mw 7.6 Bhuj earthquake, Western India. *Nat Hazards* 65:1085–1107. <https://doi.org/10.1007/s11069-011-0083-3>
- Sairam B, Singh AP, Patel V, Pancholi V, Chopra S, Dwivedi VK, Ravi Kumar M (2018) Influence of local site effects in the Ahmedabad mega city on the damage due to past earthquakes in Northwestern India. *Bull Seismol Soc Am* 108(4):2170–2182
- Schnabel PB (1973) Effects of local geology and distance from source on earthquake ground motion, Ph.D. Thesis, University of California, Berkeley, California
- Seed HB, Idriss IM (1970) Soil moduli and damping factors for dynamic response analyses, earthquake engineering research center, University of California, Berkeley, California, Rep. No. EERC-70/10
- Sharma ML, Narayan JP, Rao KS (2004) Seismic microzonation of Delhi region in India. In: 13th World Conference on Earthquake Engineering Vancouver, B.C., Canada during 1–6 Aug 2004, Paper No. 2043
- Silva W, Darragh RB (1995) Engineering characterization of strong ground motion recorded at rock sites. EPRI Report TR102262
- Singh SK, Ordaz M, Dattatrayam RS, Gupta HK (1999) A spectral analysis of the May 21, 1997, Jabalpur, India earthquake (Mw 5.8) and estimation of ground motion from future earthquakes in the Indian shield region. *Bull Seism Soc Am* 89:1620–1630
- Singh SK, Garcia D, Pacheco JF, Valenzuela R, Bansal BK, Dattatrayam RS (2004) Q of the Indian shield. *Bull Seismol Soc Am* 94(4):1564–1570
- Sitharam TG, Kolathayar S (2013) Seismic hazard analysis of India using areal sources. *J Asian Earth Sci* 62:647–653

- Sun JI, Golesorkhi R, Seed HB (1988) Dynamic moduli and damping ratios of cohesive soils. Report No.EERC 88-15, University of California, Berkeley
- Trivedi SS (2011) Soil amplification studies for Ahmedabad region. In: Proceedings International Conference on Current Trends in Technology, 'NUiCONE – 2011 held at Institute of Technology, Nirma University, Ahmedabad on 08-10 Dec 2011
- Ugurhan B, Askan A (2010) Stochastic strong ground motion simulation of the 12 November 1999 Düzce (Turkey) earthquake using a dynamic corner frequency approach. *Bull Seismol Soc Am* 100(4):1498–1512
- Wani MR, Kundu J (1995) Tectonostratigraphic analysis of Cambay rift basin: leads for future exploration. In: Proceedings First Intern. Petrol. Conference, B.R. Publishing Corporation, Delhi. pp 147–174
- Wells DL, Coppersmith KJ (1994) New empirical relationships among magnitude, rupture length, rupture width, rupture area, and surface displacement. *Bull Seismol Soc Am* 84:974–1002
- Yagi Y, Kikuchi M (2001) Western India Earthquake, website: <http://www.eic.eri.u-tokyo.ac.jp>
- Zengin E, Cakti E (2012) Scenario based ground motion simulations for Istanbul, Turkey. In: Proceedings of 15th world conference on. Earthquake engineering, 24–28 September 2012. Lisbon, Portugal, pp 24557–24566

Publisher's Note Springer Nature remains neutral with regard to jurisdictional claims in published maps and institutional affiliations.

Affiliations

Kapil Mohan¹ · Shruti Dugar¹ · Vasu Pancholi¹ · Vinay Dwivedi¹ · Sumer Chopra¹ · B. Sairam¹

✉ Kapil Mohan
kmohan@isr.res.in; kapil_geo@yahoo.co.in

¹ Institute of Seismological Research, Knowledge Corridor, Vill. Raisan, Gandhinagar 382009, India